First look at KaonLT experiment data

Richard Trotta, Tanja Horn, Garth Huber, Pete Markowitz,
Stephen Kay, Vijay Kumar, Vladimir Berdnikov, Mireille Muhoza,
Nathan Heinrich,
and the KaonLT collaboration

L/T separated data for verifying reaction mechanism

- Jlab 6 GeV data demonstrate the technique of measuring the Q^2 dependence of L/T separated cross sections at fixed x/t to test QCD Factorization
  - Consistent with expected scaling of σ_L to leading order Q^{-6} but with relatively large uncertainties

- Separated cross sections over a large range in Q^2 are essential for:
  - Testing factorization and understanding dynamical effects in both Q^2 and –t kinematics
  - Interpretation of non-perturbative contributions in experimentally accessible kinematics

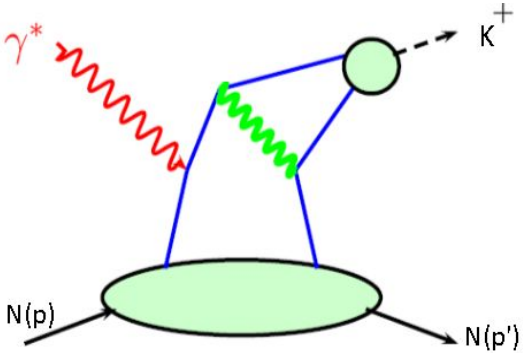

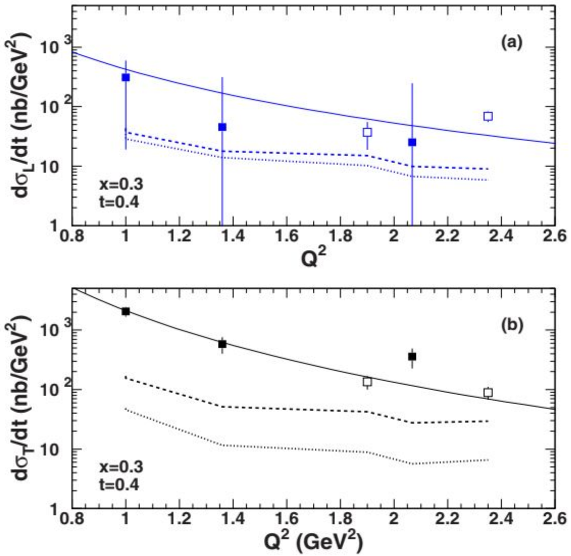

M. Carmignotto et al., PhysRevC ***97****(2018)025204*

Meson Form Factors

- Pion and kaon form factors are of special interest in hadron structure studies
  - The pion is the lightest QCD quark system and also has a central role in our understanding of the dynamic generation of mass - kaon is the next simplest system containing strangeness
- Clearest test case for studies of the transition from non-perturbative to perturbative regions
- Jlab 6 GeV data show that FF differs from hard QCD calculation evaluated with asymptotic valence-quark Distribution Amplitude (DA), but large uncertainties
- Essential for FF extractions from 12 GeV data:
  - measurements over a range of t, which would allow for interpretation of the kaon pole contribution

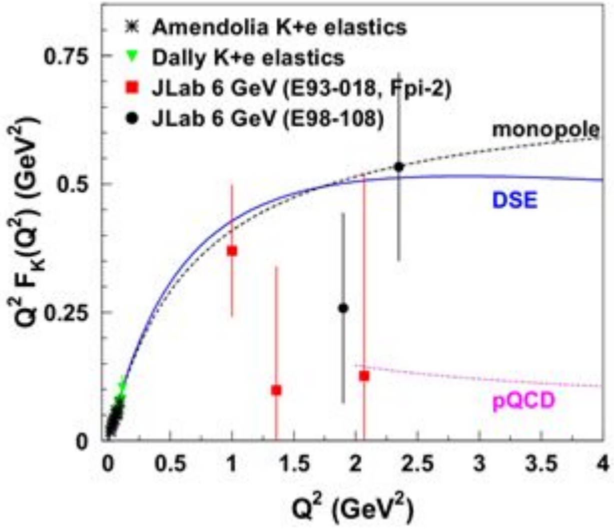

*M. Carmignotto et al., PhysRevC **97**(2018)025204*
F. Gao et al., Phys. Rev. D 96 (2017) no. 3, 034024

Experimental Determination of the π/K+ Form Factor

- At larger Q^2, $F^2_{\pi+}$ must be measured indirectly using the "pion cloud" of the proton via the p(e,e'π^+)n process
  - At small –t, the pion pole process dominates the longitudinal cross section, σ_L
  - In the Born term model, $F^2_{\pi+}$ appears as

$$\frac{d\sigma_L}{dt} \propto \frac{-t}{(t-m_\pi^2)} g_{\pi NN}^2(t) Q^2 F_\pi^2(Q^2,t)$$

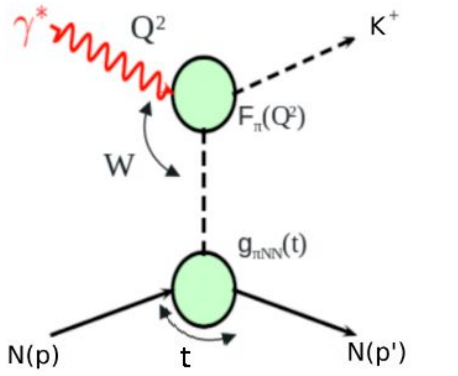

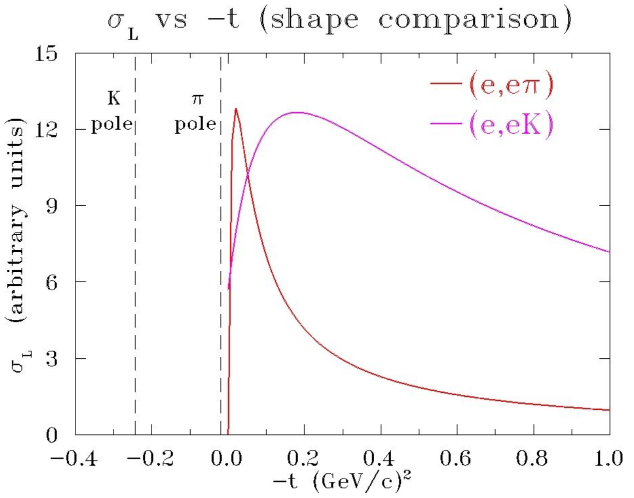

- Requirements:
  - Full L/T separation of the cross section – isolation of σ_L
  - Selection of the pion pole process
  - Extraction of the form factor using a model
  - Validation of the technique - model dependent checks

L/T Separation Example

- σ_L is isolated using the Rosenbluth separation technique
- Measure the cross section at two beam energies and fixed W, Q^2, -t
- Simultaneous fit using the measured azimuthal angle (ϕ) allows for extracting L, T, LT, and TT
  - Careful evaluation of the systematic uncertainties is important due to the 1/ε amplification in the σL extraction
  - Spectrometer acceptance, kinematics, and efficiencies
- Magnetic spectrometers a must for such precision cross section measurements
  - This is only possible in Hall C at JLab

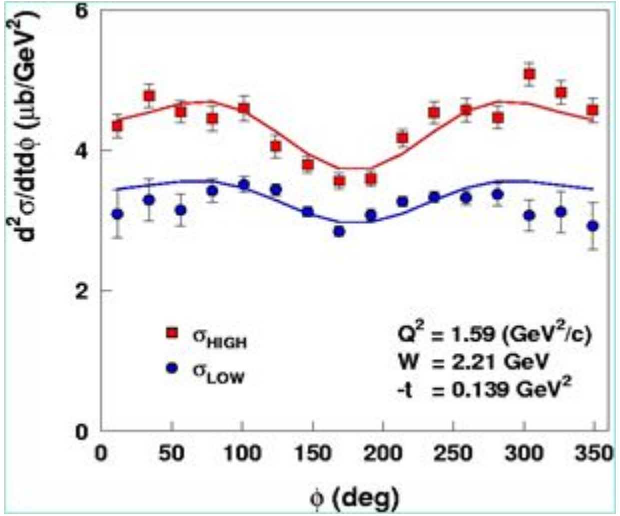

$$2\pi\frac{d^2\sigma}{dtd\phi} = \varepsilon\frac{d\sigma_L}{dt} + \frac{d\sigma_T}{dt} + \sqrt{2\varepsilon(\varepsilon+1)}\,\frac{d\sigma_{LT}}{dt}\cos\phi + \varepsilon\frac{d\sigma_{TT}}{dt}\cos 2\phi$$

σ_L will give us F^2_{K+}

L/T Separation Example

$$2\pi\frac{d^2\sigma}{dt\,d\phi} = \varepsilon\frac{d\sigma_L}{dt} + \frac{d\sigma_T}{dt} + \sqrt{2\varepsilon(\varepsilon+1)}\,\frac{d\sigma_{LT}}{dt}\cos\phi + \varepsilon\frac{d\sigma_{TT}}{dt}\cos 2\phi$$

Physics cross section

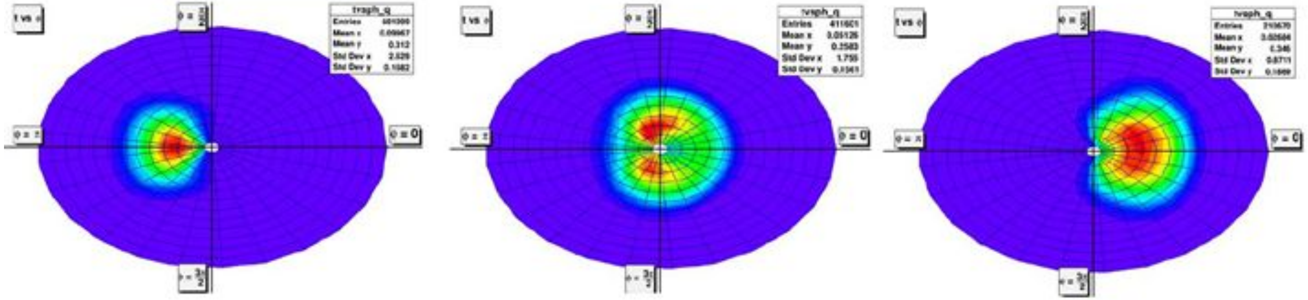

- Three SHMS angles for azimuthal (ϕ) coverage to determine the interference terms (LT, TT)
- Two beam energies (ε) to separate longitudinal (L) from transverse (T) cross section

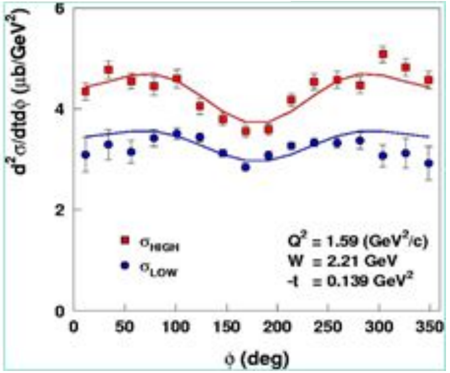

Fit using measured ε and ϕ dependence

Review E12-09-011 (KaonLT) Goals

- The Q^2 dependence will allow studying the scaling behavior of the separated cross sections
  - First cross section data for Q^2 scaling tests with kaons
  - Highest Q^2 for L/T separated kaon electroproduction cross section
  - First separated kaon cross section measurement above W=2.2 GeV

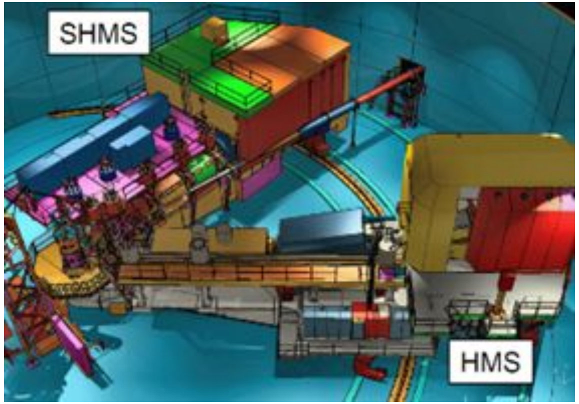

- The t-dependence allows for detailed studies of the reaction mechanism
  - Contributes to understanding of the non-pole contributions, which should reduce the model dependence in interpreting the data
  - Bonus: if warranted by data, extract the kaon form factor

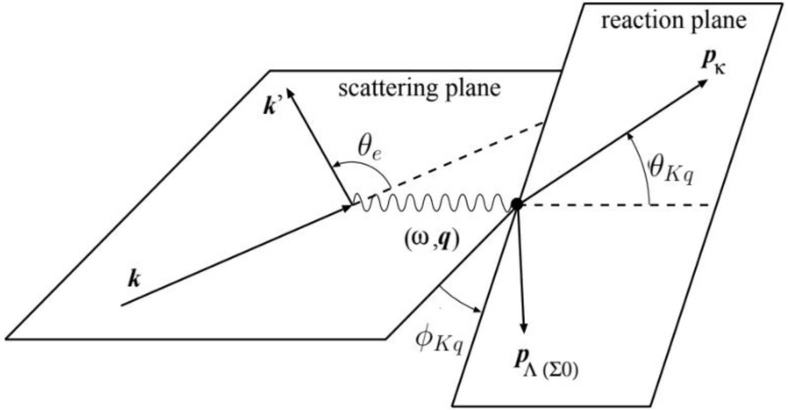

Kaon LT - Data Collected

- The $p(e, e'K^+)\Lambda,\Sigma^0$ experiment ran in Hall C at Jefferson Lab over the fall and spring.

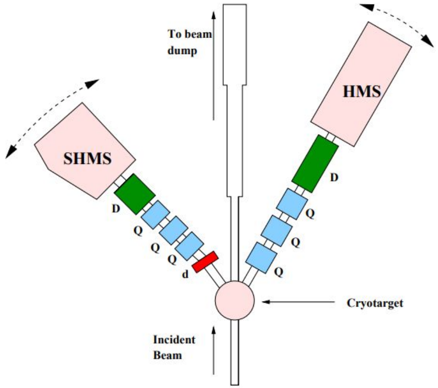

E (GeV)	Q^2 (GeV^2)	W (GeV)	x	ε_{high}	ε_{low}
10.6/6.2	3.0	2.32	0.40	0.88	0.57
10.6/6.2	2.115	2.95	0.21	0.79	0.25
10.6/8.2	4.4	2.74	0.40	0.72	0.48
10.6/8.2	3.0	3.14	0.25	0.67	0.39
10.6/8.2	5.5	3.02	0.40	0.53	0.18
4.9/3.8	0.5	2.40	0.09	0.70	0.45

Experimental Details

- Hall C: k_e=3.8, 4.9, 6.4, 8.5, 10.6 GeV
- SHMS for kaon detection :
  - Kaon angles between 6 – 30 deg
  - Kaon momenta between 2.7 – 6.8 GeV/c
- HMS for electron detection :
  - angles between 10.7 – 31.7 deg
  - momenta between 0.86 – 5.1 GeV/c
- Particle identification:
  - Dedicated Aerogel Cherenkov detector for kaon/proton separation
    - Four refractive indices to cover the dynamic range required by experiments
  - Heavy gas Cherenkov detector for kaon/pion separation

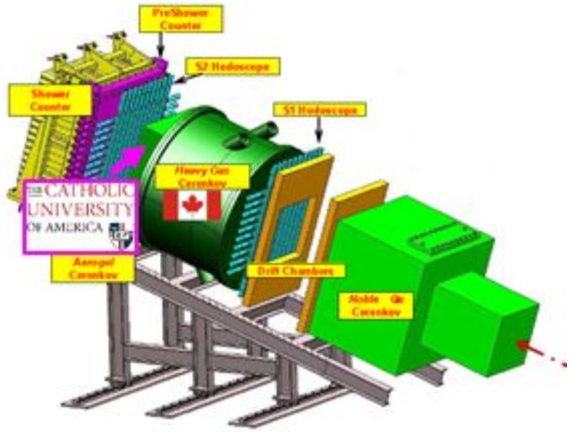

n	π_{thr} (GeV/c)	K_{thr} (GeV/c)	P_{thr} (GeV/c)
1.030	0.57	2.00	3.80
1.020	0.67	2.46	4.67
1.015	0.81	2.84	5.40
1.011	0.94	3.32	6.31

SHMS small angle operation

- Some issues with opening and small angle settings at beginning of run, but SHMS at 6.01° and HMS at 12.7° on 12/17/18

Work of many people...

KaonLT Event Selection

- Isolate Exclusive Final States through missing mass

$$M_x = \sqrt{(E_det - E_init)^2 - (p_det - p_init)^2}$$

- Coincidence measurement between kaons in SHMS and electrons in HMS
  - simultaneous studies of KΛ and $K\Sigma^0$ channels…and a few others…
- Kaon pole dominance tests through

$$\frac{\sigma_L(\gamma^* p \rightarrow K^+\Sigma^0)}{\sigma_L(\gamma^* p \rightarrow K^+\Lambda)}$$

  - Should be similar to ratio of coupling constants $g^2_{pK\Lambda}/g^2_{pK\Sigma}$ if t-channel

Online data

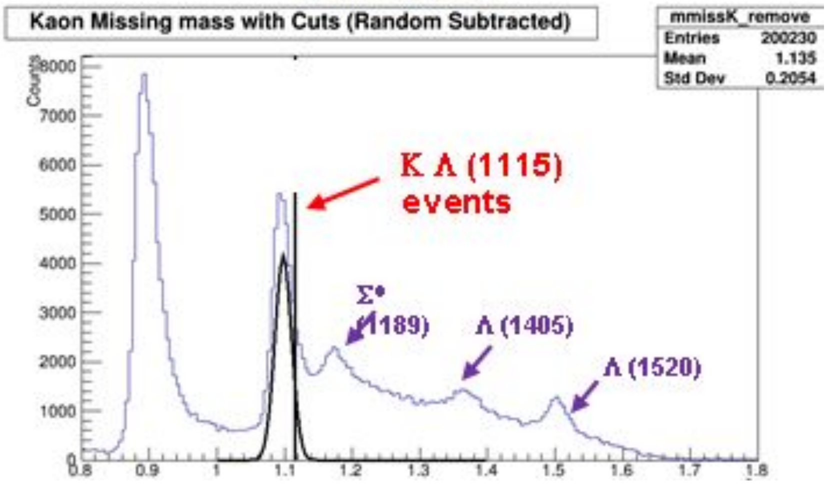

Interesting Physics in the other channels

- Large difference in L/T ratio between p(e.e’π^+)n and p(e,e’π^+)Δ^0 final states – G. Huber hclog #3640187

KaonLT: Q^2=0.50 GeV^2

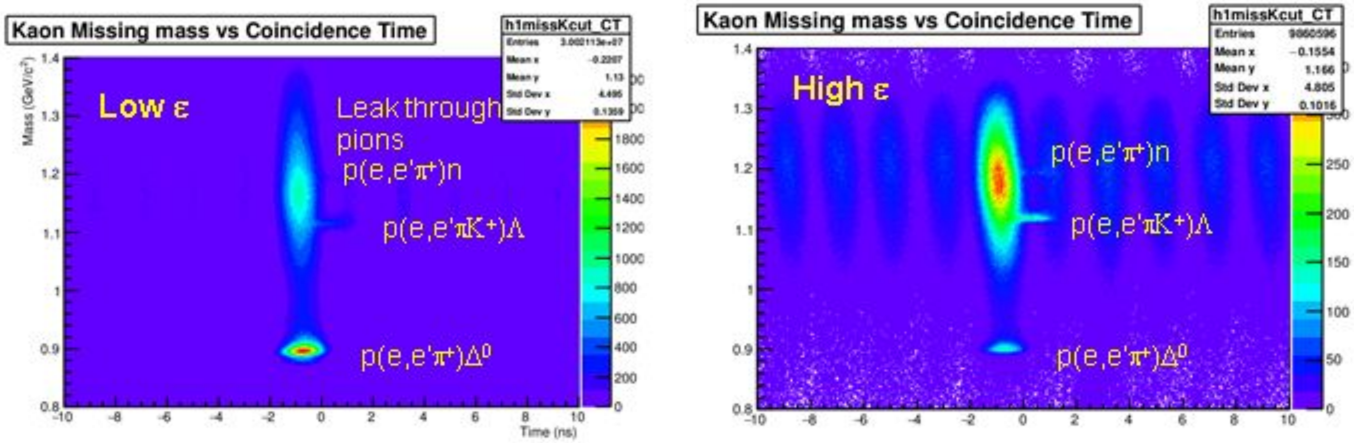

- Large increase in neutron missing mass at high epsilon is evidence of the pion-pole process at low Q^2 and small –t, which suggests $\sigma_L >> \sigma_T$
- Δ^0 exclusive longitudinal cross section expected to be at best $\sigma_L \sim \sigma_T$

Comparison of high and low epsilon

- Q^2=3.0, W=2.32, x=0.40
- [10.6 Gev (high ε), 6.2 Gev (low ε)]
- Left (θ_{high}=21.18,θ_{low}=16.28)

10.6 GeV (high ε)

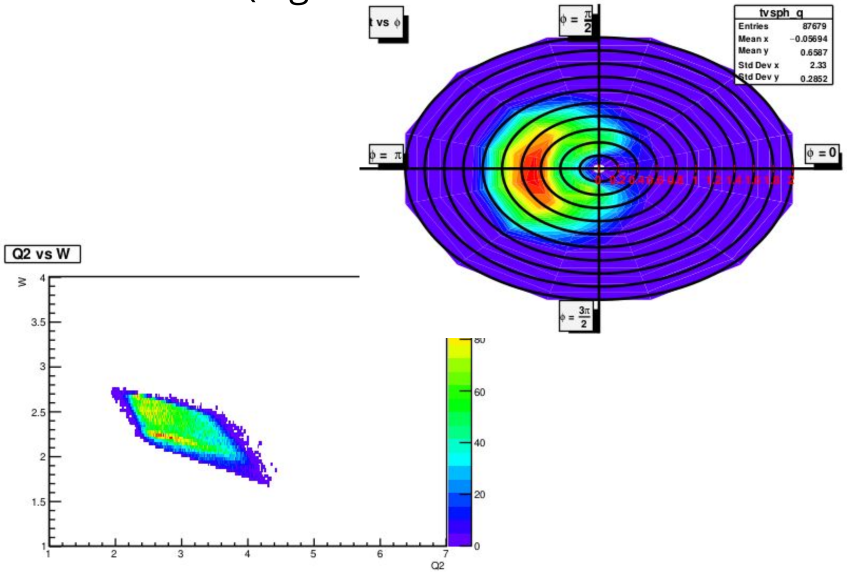

6.2 GeV (low ε)

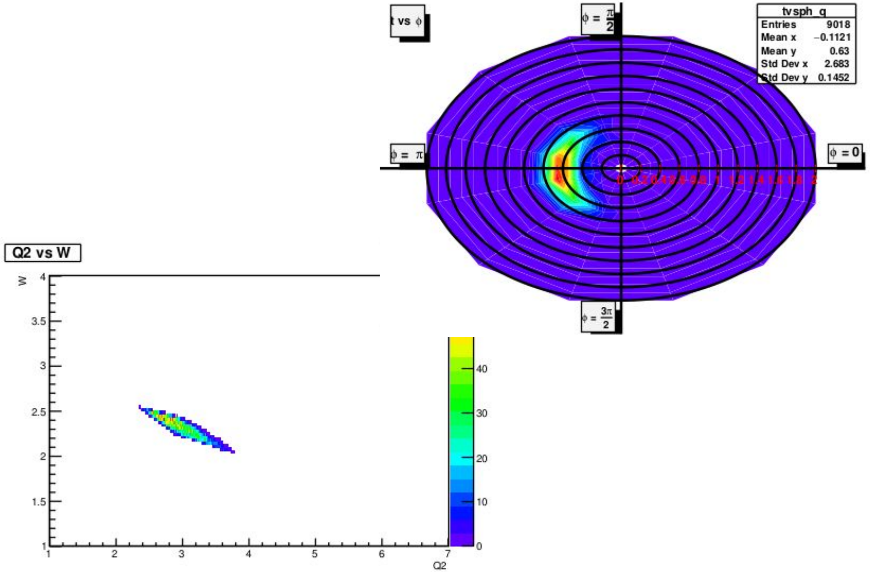

Comparison of high and low epsilon

- Q^2=3.0, W=2.32, x=0.40
- [10.6 Gev (high ε), 6.2 Gev (low ε)]
- Left (θ_{high}=21.18,θ_{low}=16.28)

10.6 GeV (high ε)

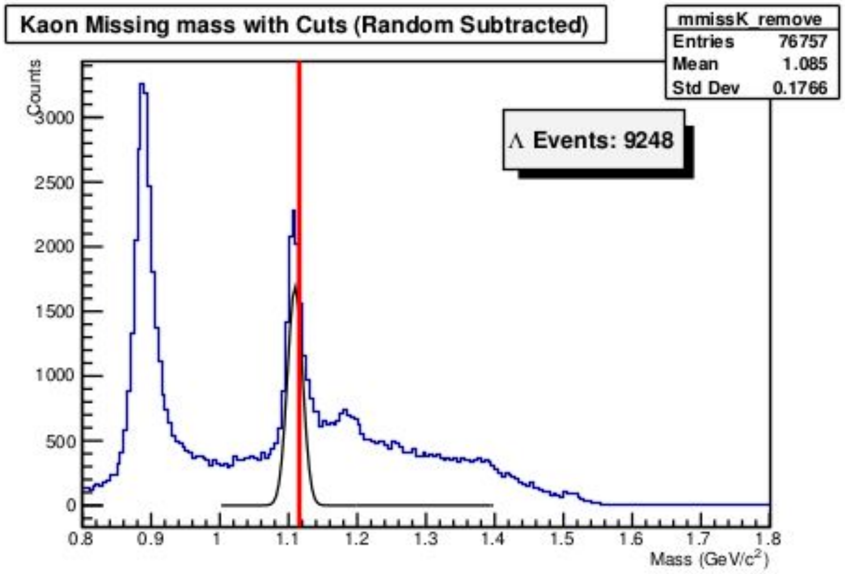

6.2 GeV (low ε)

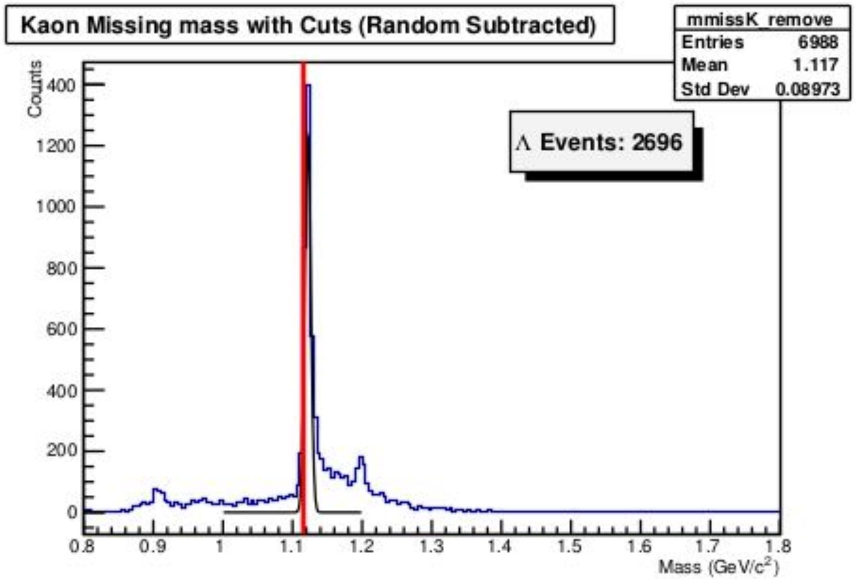

Comparison of high and low epsilon

- Q^2=3.0, W=3.14, x=0.25
- [10.6 Gev (high ε), 8.2 Gev (low ε)]
- Center (θ_{high}=9.42,θ_{low}=6.89)

10.6 GeV (high ε)

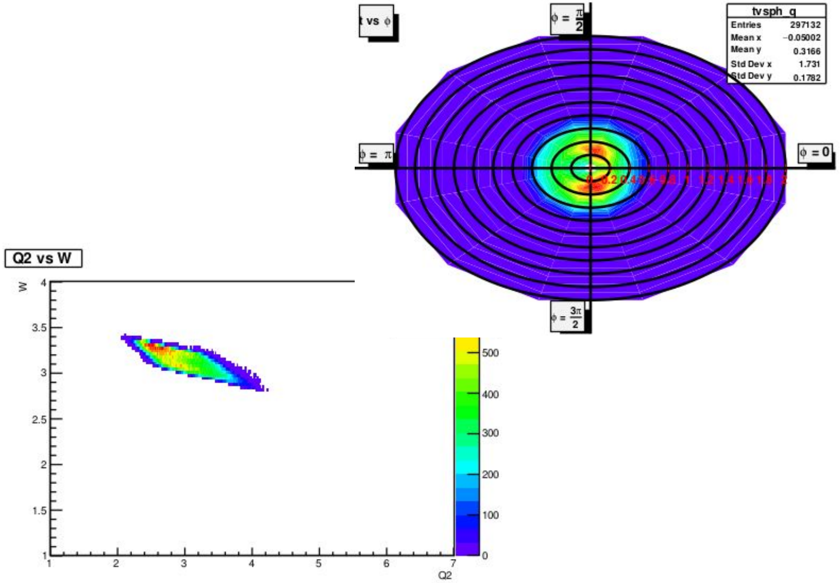

8.2 GeV (low ε)

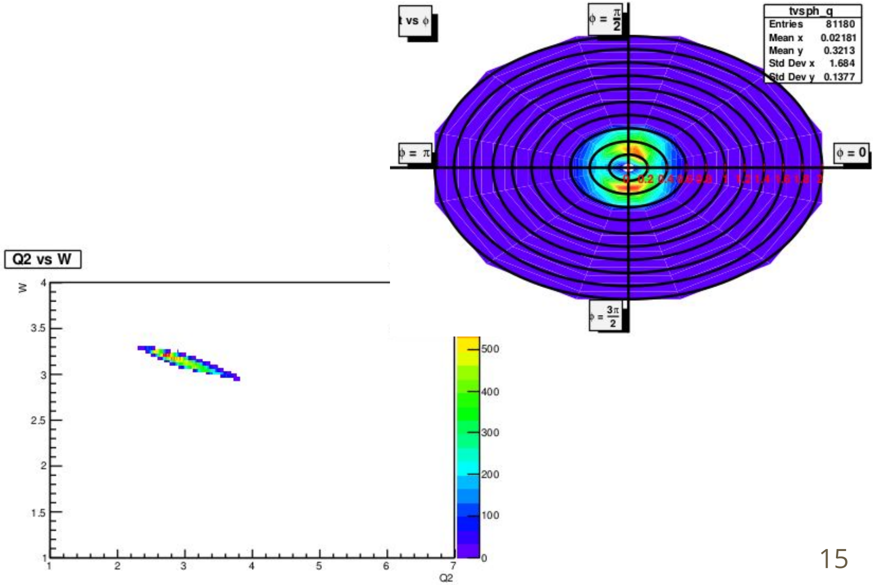

Comparison of high and low epsilon

- Q^2=3.0, W=3.14, x=0.25
- [10.6 Gev (high ε), 8.2 Gev (low ε)]
- Center (θ_{high}=9.42,θ_{low}=6.89)

10.6 GeV (high ε)

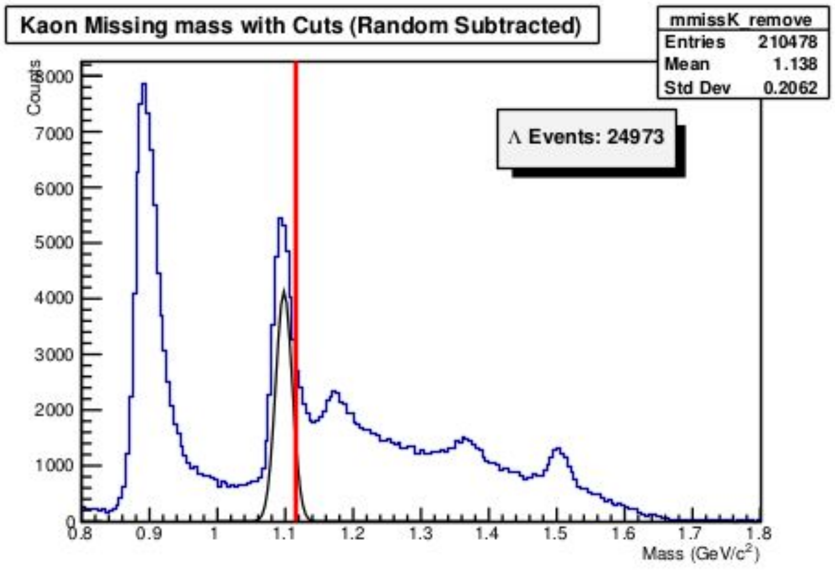

8.2 GeV (low ε)

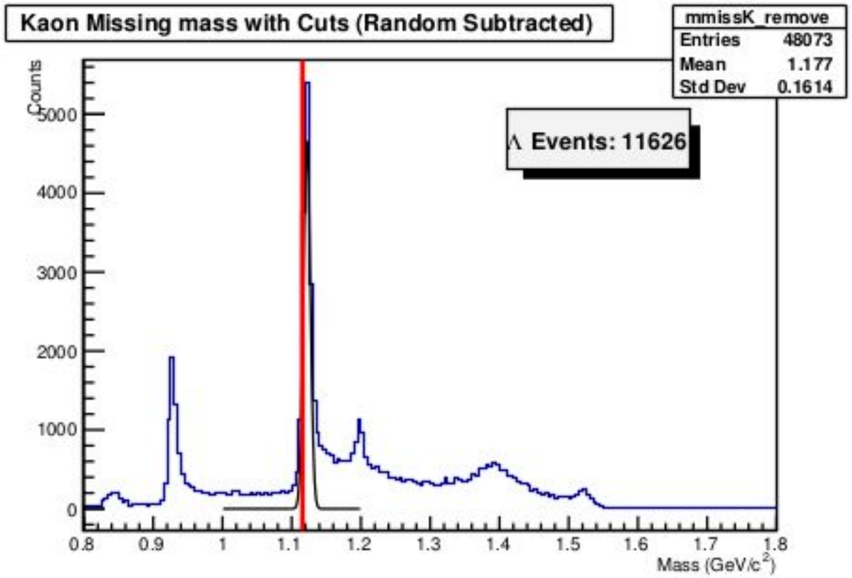

Comparison of high and low epsilon

- Q^2=3.0, W=3.14, x=0.25
- [10.6 Gev (high ε)]
- Right (θ_{high}=6.65)

10.6 GeV (high ε)

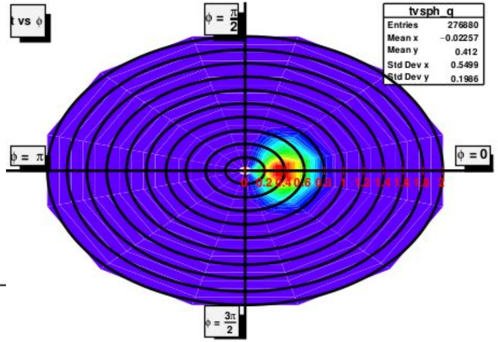

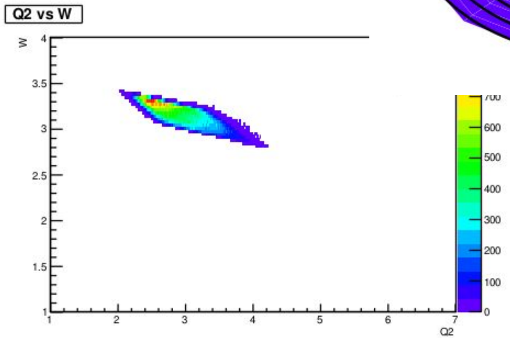

Comparison of high and low epsilon

- Q^2=3.0, W=3.14, x=0.25
- [10.6 Gev (high ε)]
- Right (θ_{high}=6.65)

10.6 GeV (high ε)

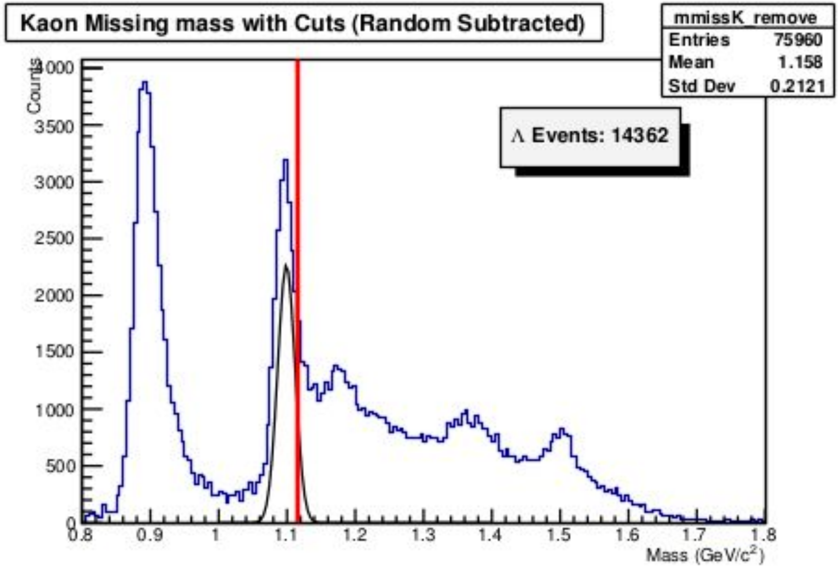

Comparison of high and low epsilon

- Q^2=0.5, W=2.40, x=0.09
- [4.9 Gev (high ε), 3.8 Gev (low ε)]
- Center (θ_{high}=8.86,θ_{low}=6.79)

4.9 GeV (high ε)

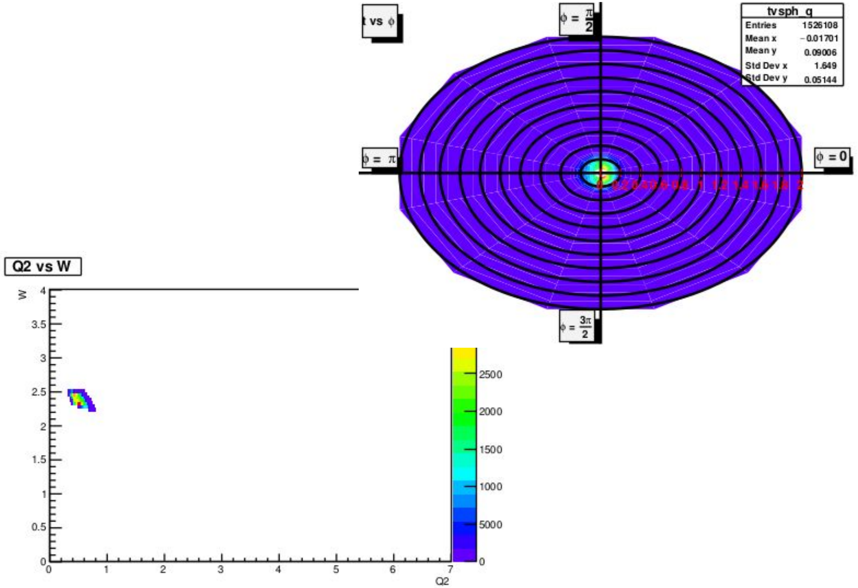

3.8 GeV (low ε)

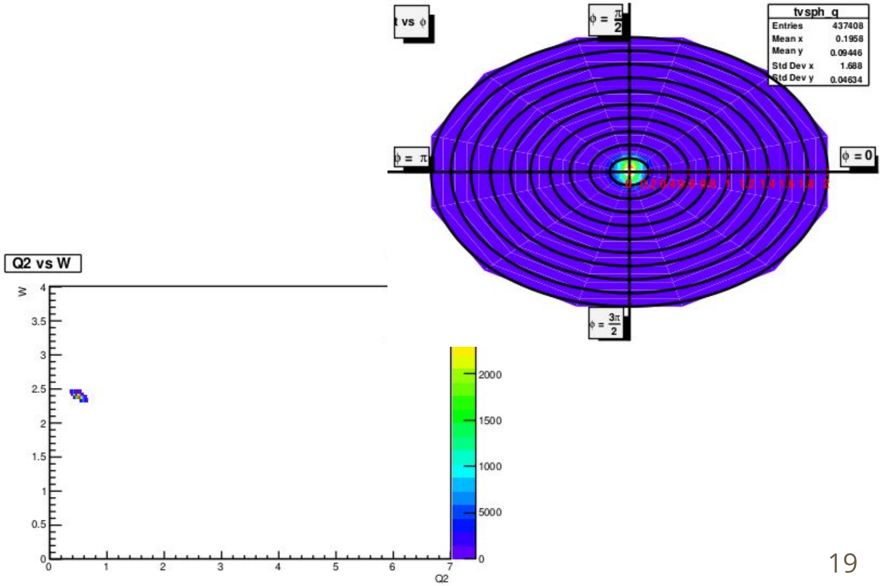

Comparison of high and low epsilon

- Q^2=0.5, W=2.40, x=0.09
- [4.9 Gev (high ε), 3.8 Gev (low ε)]
- Center (θ_{high}=8.86,θ_{low}=6.79)

4.9 GeV (high ε)

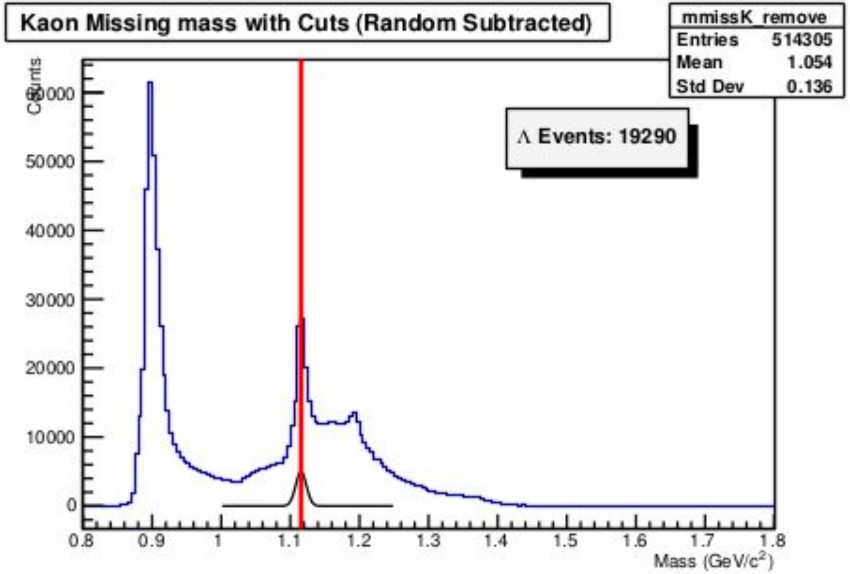

3.8 GeV (low ε)

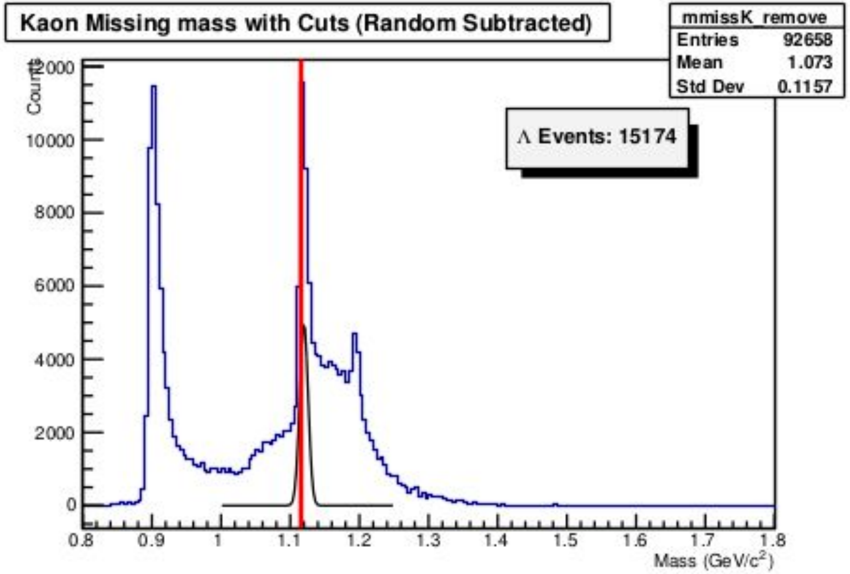

Analysis Phases

1. Calibrations
   - Calorimeter, aerogel, HC cer, HMS cer, DC, Quartz plan of hodo
   - Assure we are replaying to optimize our physics settings
2. Efficiencies and offsets
   - Luminosity and elastics
3. First iteration of cross section
   - Bring everything together
4. Fine tune
   - Fine tune values to minimize systematics
5. Repeat previous step
   - Repeat until acceptable cross sections are reached
6. Possible attempt at form factor extraction
   - Fit the data to a model and iterate

Current Phase

- Understanding efficiencies from luminosity scans has been ongoing with only one run having been looked at
- In the process of calibrations
- Once calibrations are complete, I will concentrate on elastics studies along with continued studied of luminosity
- Should finish phase one by middle of summer

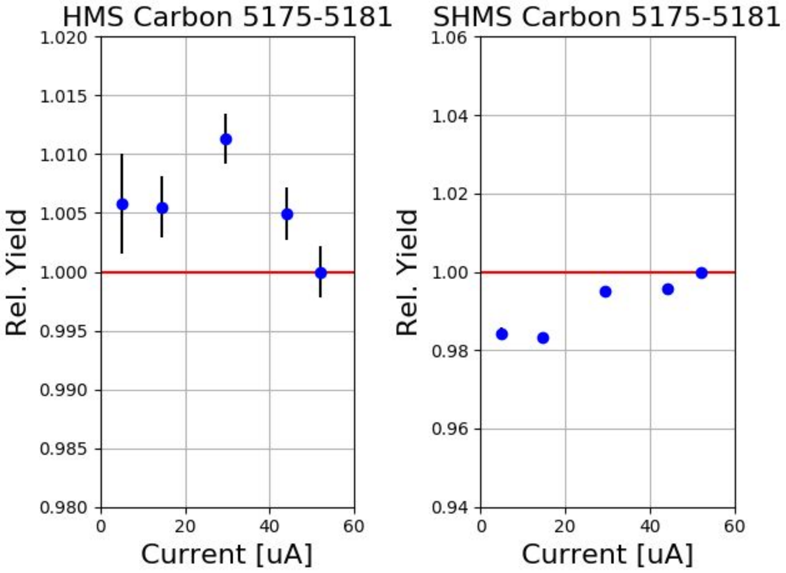

Calibration of HGC Detector (SHMS)

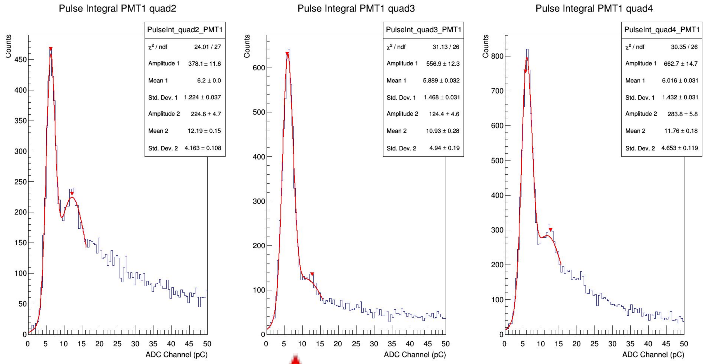

To see the second & third photo-electron, we fitted the scaled histogram with Poisson function and subtracted the higher photo-electron.

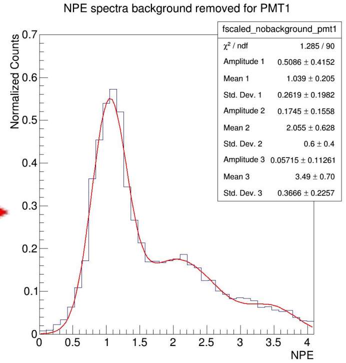

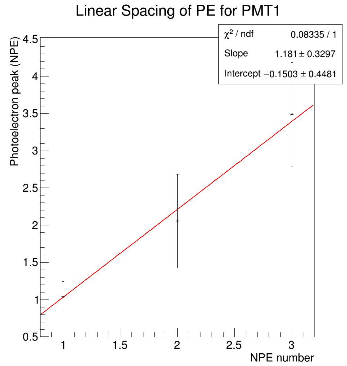

Showing the SPE in HGC for PMT1 FADC and fit it with a Gaussian function to get the mean of peaks.

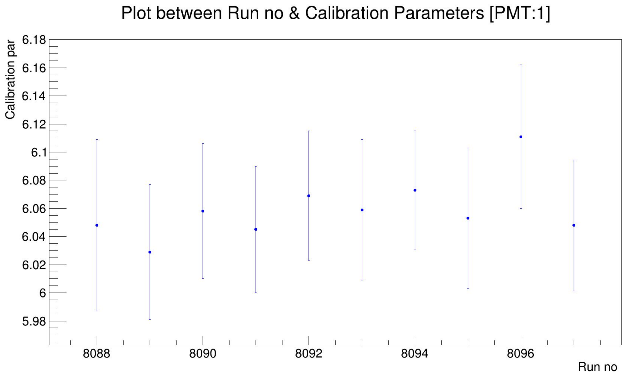

Run dependence of calibration parameters for the PMT1 to check the consistency of calibration.

HGC Timing Study

- In addition to main timing peak at +10ns, there is an unexpected second peak at -10ns.
- To better understand the origin of the unexpected peak, plot b/w Timing vs Amplitude.
    - 2nd peak corresponds to small pulses only.
- We also checked the tracking position in focal plane coordinates.
    - Interesting correlation between hit position and timing remains a mystery.

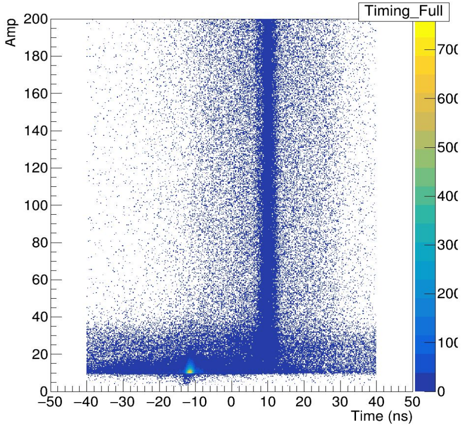

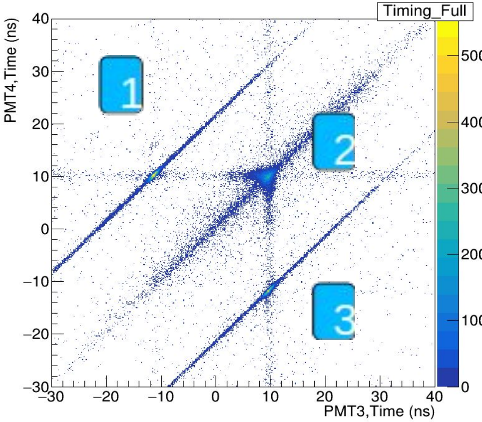

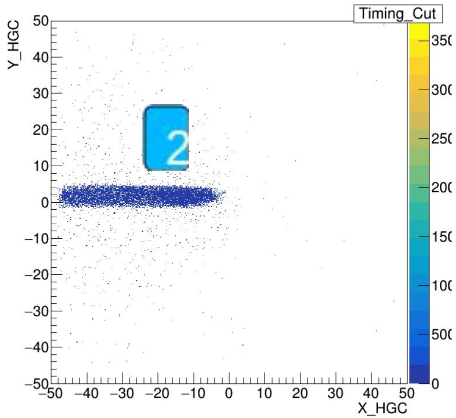

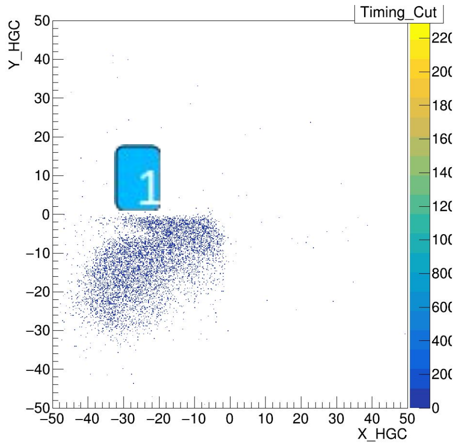

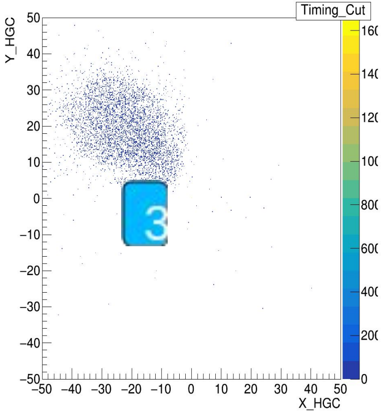

Conclusion

- Kaon can provide an interesting way to expand previous data of charged pion form factor data with access to the production mechanism involving strangeness
- E12-09-011 has completed its 2018-19 run
- Potential to extract the Kaon form factor from the L/T separated cross sections to the highest Q^2 achievable at Jlab
    - Full azimuthal coverage, good phase space matching and favorable rates to allow Kaon cross section separation
- Provide much needed data for Q^2 scaling at fixed x and -t in Kaon electroproduction to validate QCD factorization for hadron imaging studies
- Currently in the first phase of analysis with hopes of finishing by the middle of this summer

Extra Slides

KaonLT Sample Projections

- E12-09-011: Separated L/T/LT/TT cross section over a wide range of Q^2 and t

E12-09-011 spokespersons: T. Horn, G. Huber, P. Markowitz

- JLab 12 GeV Kaon Program features:
  - First cross section data for Q^2 scaling tests with kaons
  - Highest Q^2 for L/T separated kaon electroproduction cross section
  - First separated kaon cross section measurement above W=2.2 GeV

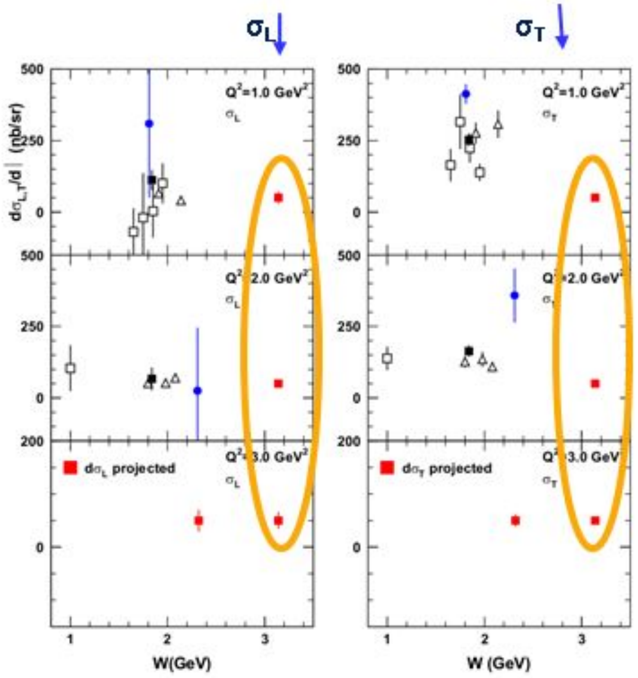

blue points from M. Carmignotto, PhD thesis (2017)

KaonLT: Projections for $F_{K+}(Q^2)$ Measurements

- E12-09-011: primary goal L/T separated kaon cross sections to investigate hard-soft factorization and non-pole contributions
- Possible K^+ form factor extraction to highest possible Q^2 achievable at JLab
  - Extraction like in the pion case by studying the model dependence at small t
  - Comparative extractions of F^2_π at small and larger t show only modest model dependence
    - larger t data lie at a similar distance from pole as kaon data

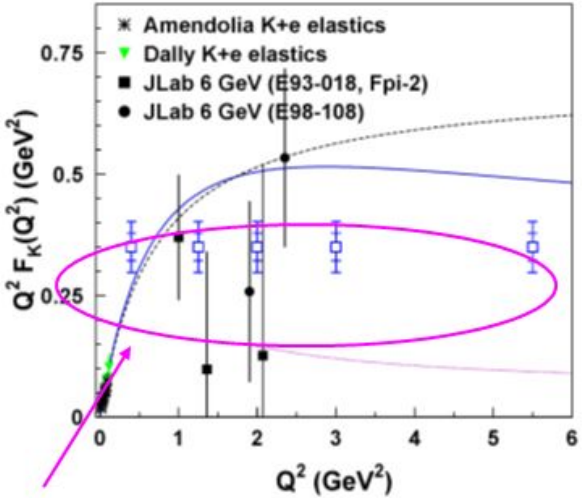

Possible extractions from 2018/19 run

Separating the Cross Section

$p(e, e'K^+)\Lambda(\Sigma^0)$

- It is crucial that full azimuthal coverage is achieved to allow further simplification using the Rosenbluth separation technique.
  - Rosenbluth separation involves measuring the terms over full 2π azimuthal coverage and integrating over the experimental acceptance to eliminate any interference terms.

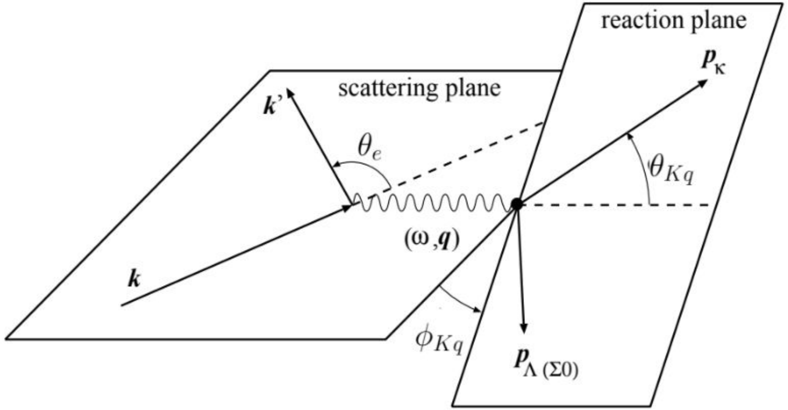

$$2\pi\frac{d^2\sigma}{dt\,d\phi} = \varepsilon\frac{d\sigma_L}{dt} + \frac{d\sigma_T}{dt} + \sqrt{2\varepsilon(\varepsilon+1)}\,\frac{d\sigma_{LT}}{dt}\cos\phi + \varepsilon\frac{d\sigma_{TT}}{dt}\cos 2\phi$$

Comparison of high and low epsilon

- Q^2=3.0, W=2.32, x=0.40
- [10.6 Gev (high ε), 6.2 Gev (low ε)]
- Center (θ_{high}=18.18,θ_{low}=13.28)

10.6 GeV (high ε)

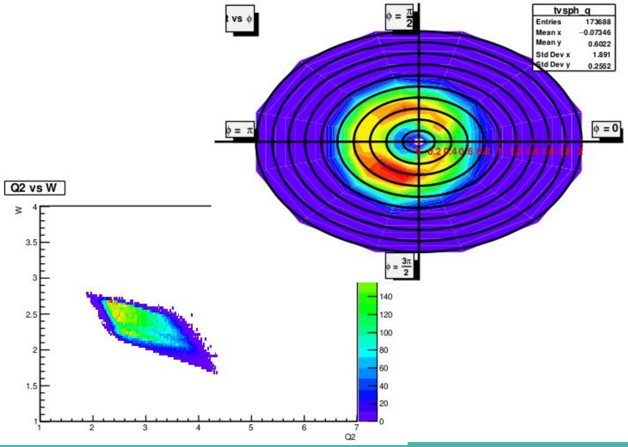

6.2 GeV (low ε)

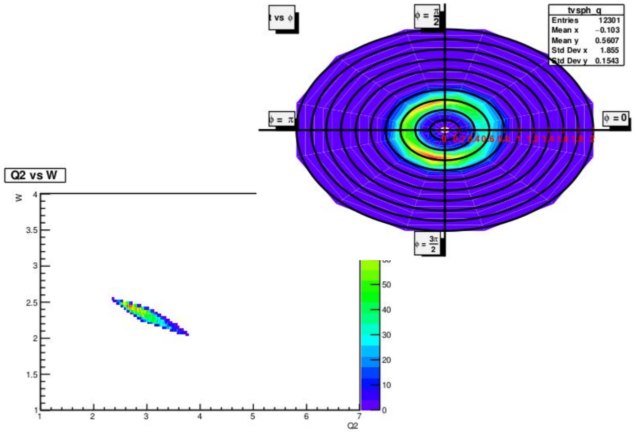

Comparison of high and low epsilon

- Q^2=3.0, W=2.32, x=0.40
- [10.6 Gev (high ε), 6.2 Gev (low ε)]
- Center (θ_{high}=18.18,θ_{low}=13.28)

10.6 GeV (high ε)

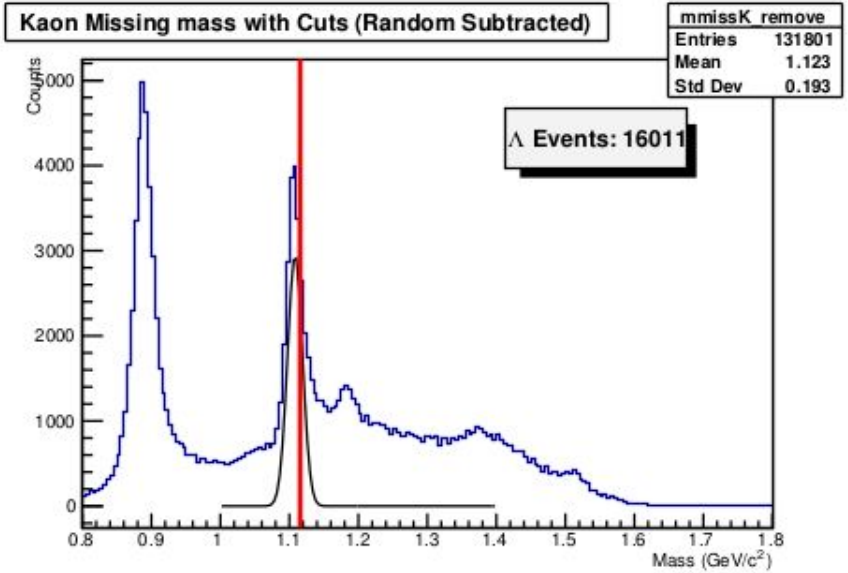

6.2 GeV (low ε)

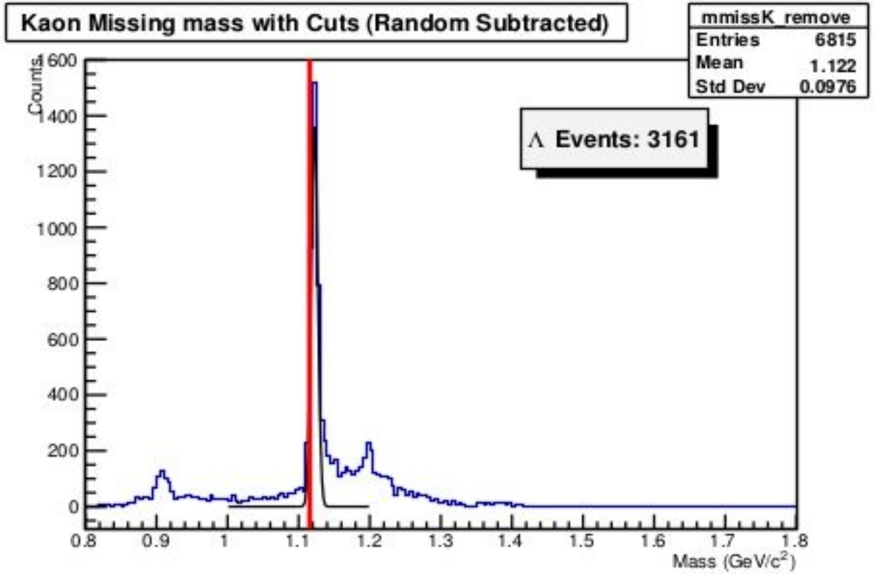

Comparison of high and low epsilon

- Q^2=3.0, W=2.32, x=0.40
- [10.6 Gev (high ε)]
- Right (θ_{high}=15.18)

10.6 GeV (high ε)

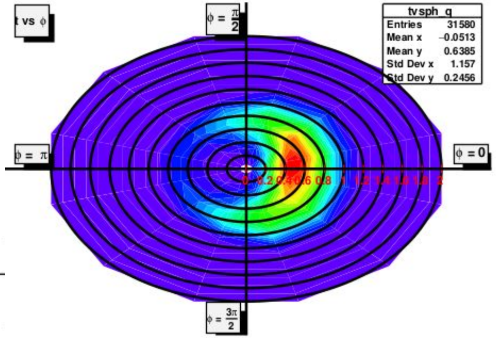

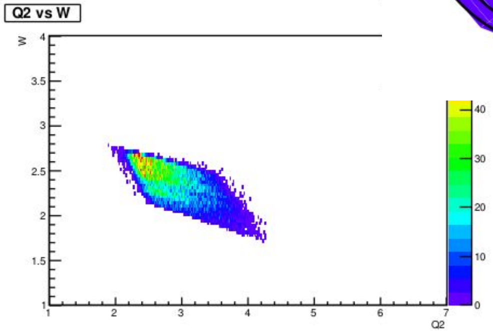

Comparison of high and low epsilon

- Q^2=3.0, W=2.32, x=0.40
- [10.6 Gev (high ε)]
- Right (θ_{high}=15.18)

10.6 GeV (high ε)

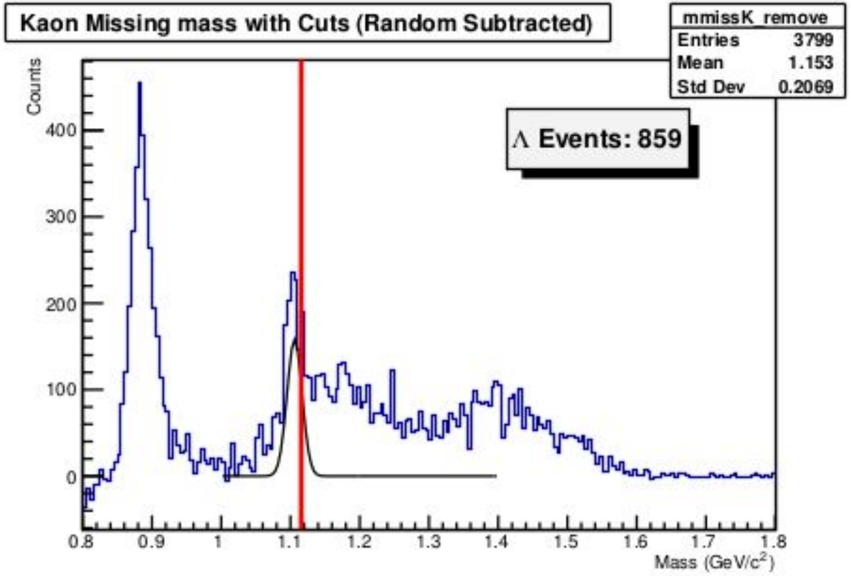

Comparison of high and low epsilon

- Q^2=2.115, W=2.95, x=0.21
- [10.6 Gev (high ε), 6.2 Gev (low ε)]
- Center (θ_{high}=10.74,θ_{low}=6.20)

10.6 GeV (high ε)

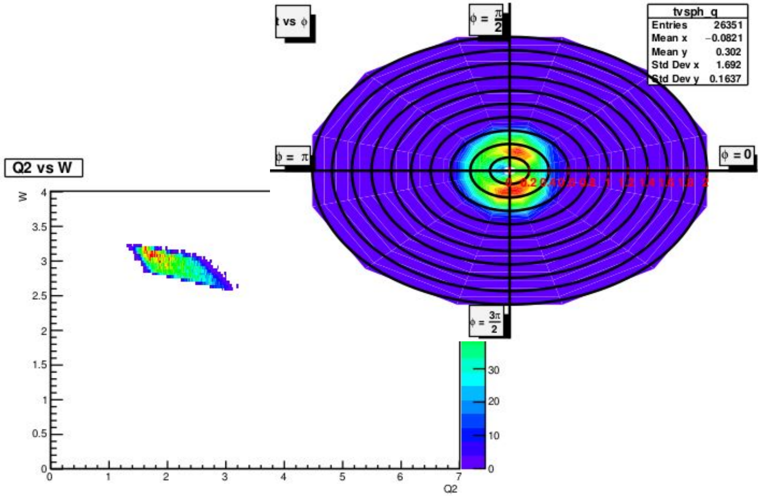

6.2 GeV (low ε)

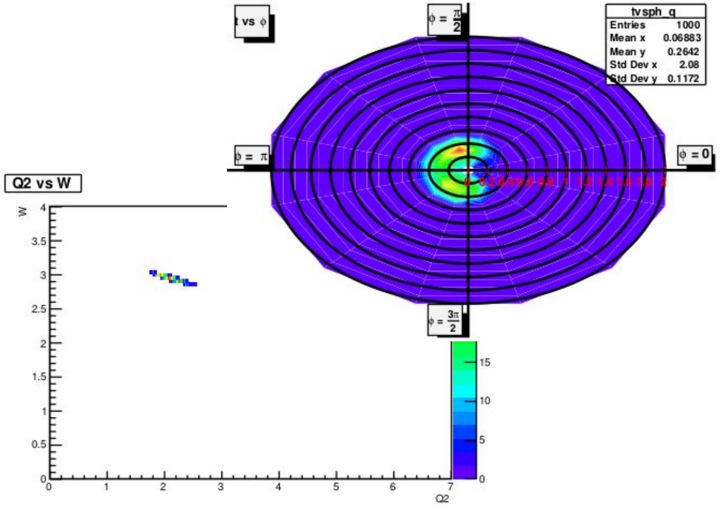

Comparison of high and low epsilon

- Q^2=2.115, W=2.95, x=0.21
- [10.6 Gev (high ε), 6.2 Gev (low ε)]
- Center (θ_{high}=10.74,θ_{low}=6.20)

10.6 GeV (high ε)

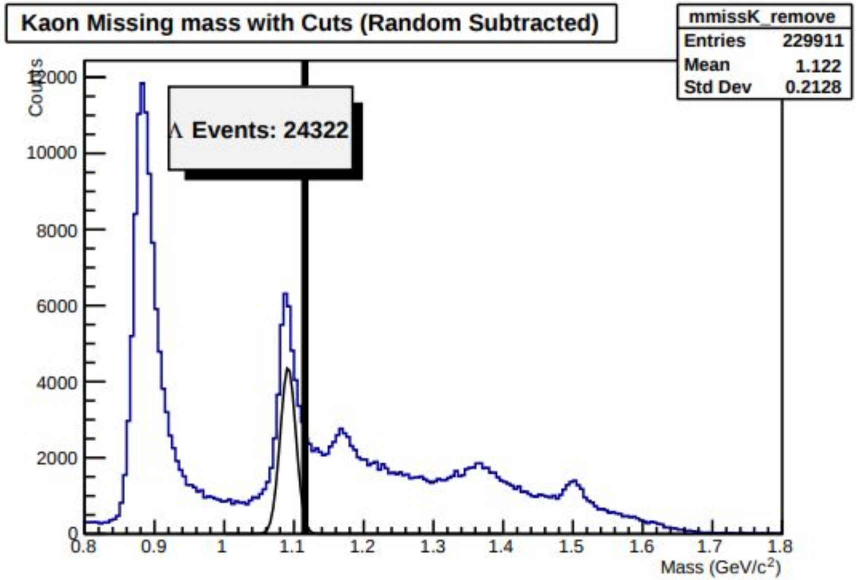

6.2 GeV (low ε)

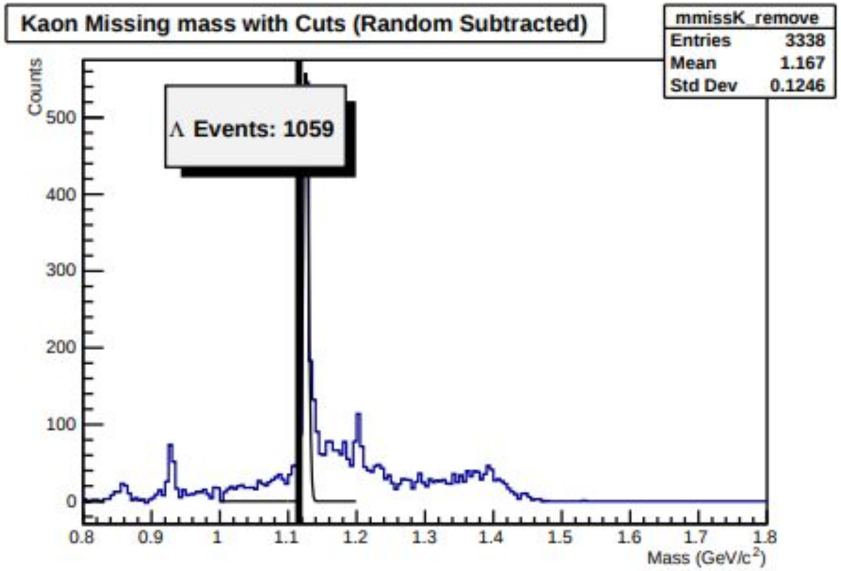

Comparison of high and low epsilon

- Q^2=2.115, W=2.95, x=0.21
- [10.6 Gev (high ε), 6.2 Gev (low ε)]
- Left (θ_{high}=13.74,θ_{low}=8.48)

10.6 GeV (high ε)

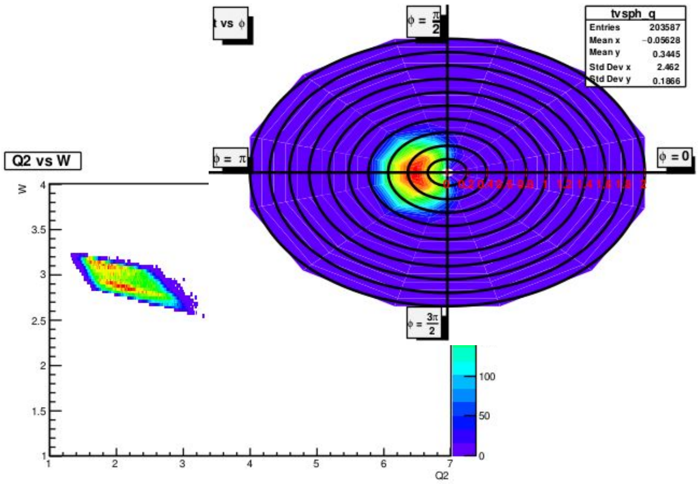

6.2 GeV (low ε)

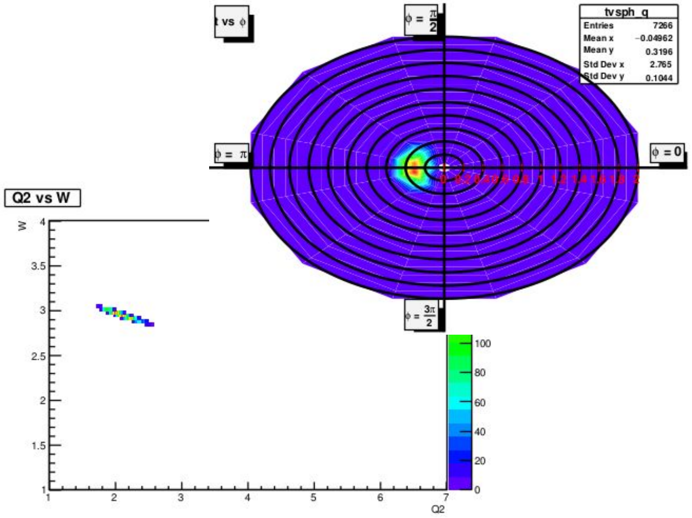

Comparison of high and low epsilon

- Q^2=2.115, W=2.95, x=0.21
- [10.6 Gev (high ε), 6.2 Gev (low ε)]
- Left (θ_{high}=13.74,θ_{low}=8.48)

10.6 GeV (high ε)

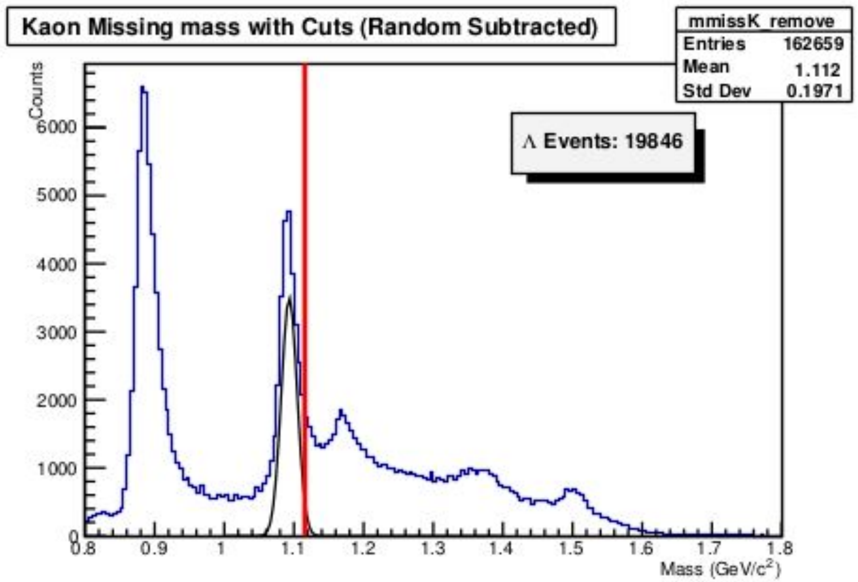

6.2 GeV (low ε)

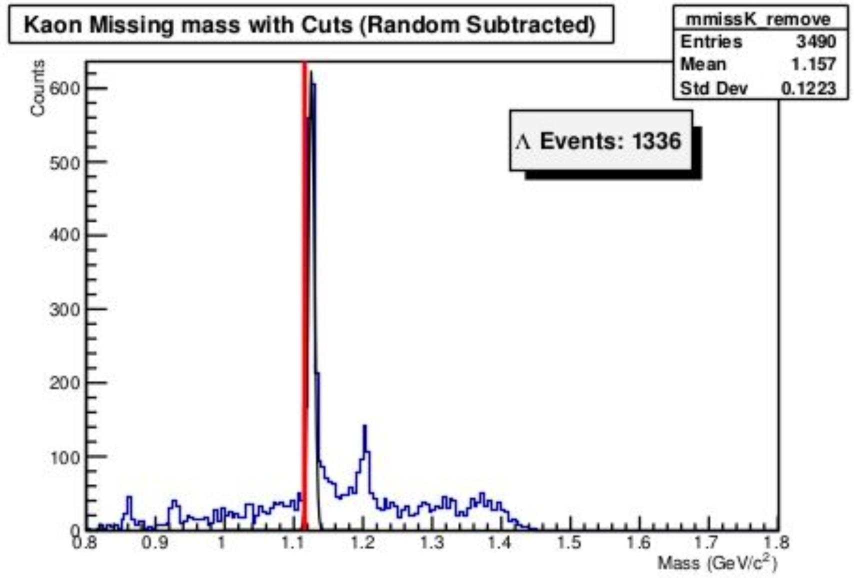

Comparison of high and low epsilon

- Q^2=2.115, W=2.95, x=0.21
- [10.6 Gev (high ε)]
- Right (θ_{high}=7.74)

10.6 GeV (high ε)

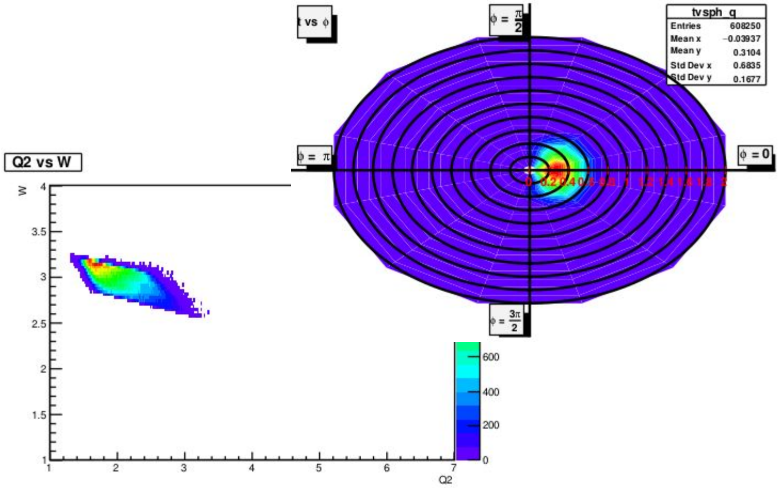

Comparison of high and low epsilon

- Q^2=2.115, W=2.95, x=0.21
- [10.6 Gev (high ε)]
- Right (θ_{high}=7.74)

10.6 GeV (high ε)

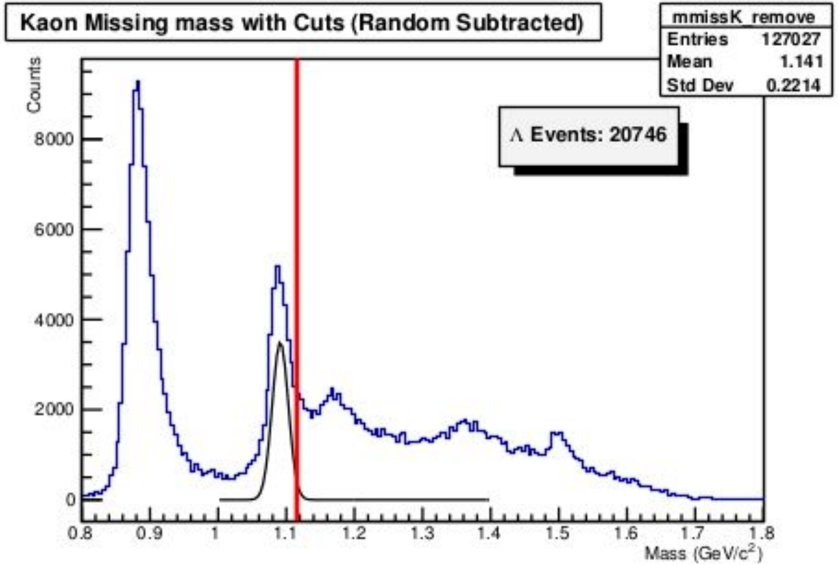

Comparison of high and low epsilon

- Q^2=4.4, W=2.74, x=0.40
- [10.6 Gev (high ε), 8.2 Gev (low ε)]
- Center (θ_{high}=12.81,θ_{low}=10.00)

10.6 GeV (high ε)

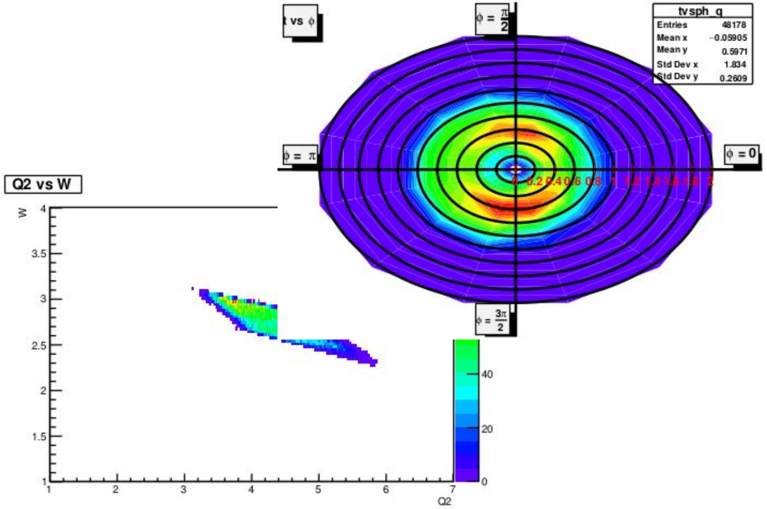

8.2 GeV (low ε)

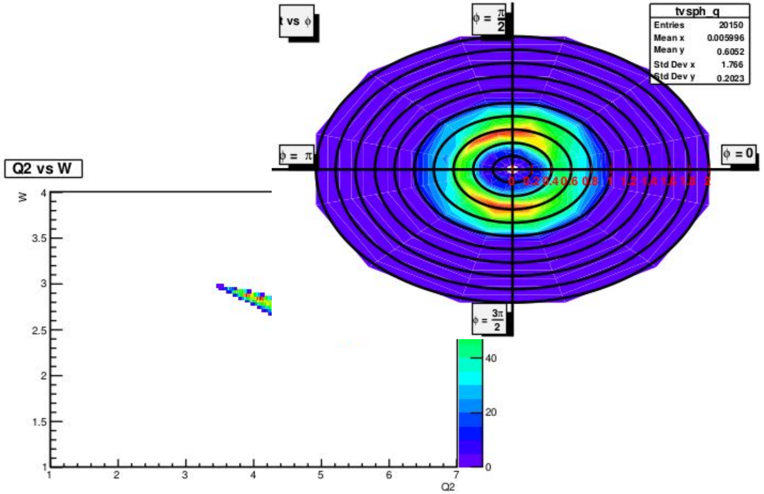

Comparison of high and low epsilon

- Q^2=4.4, W=2.74, x=0.40
- [10.6 Gev (high ε), 8.2 Gev (low ε)]
- Center (θ_{high}=12.81,θ_{low}=10.00)

10.6 GeV (high ε)

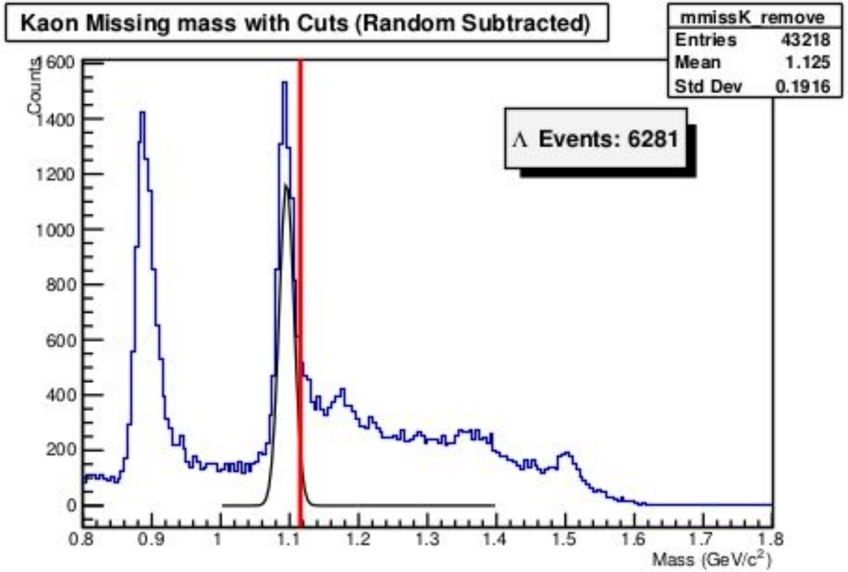

8.2 GeV (low ε)

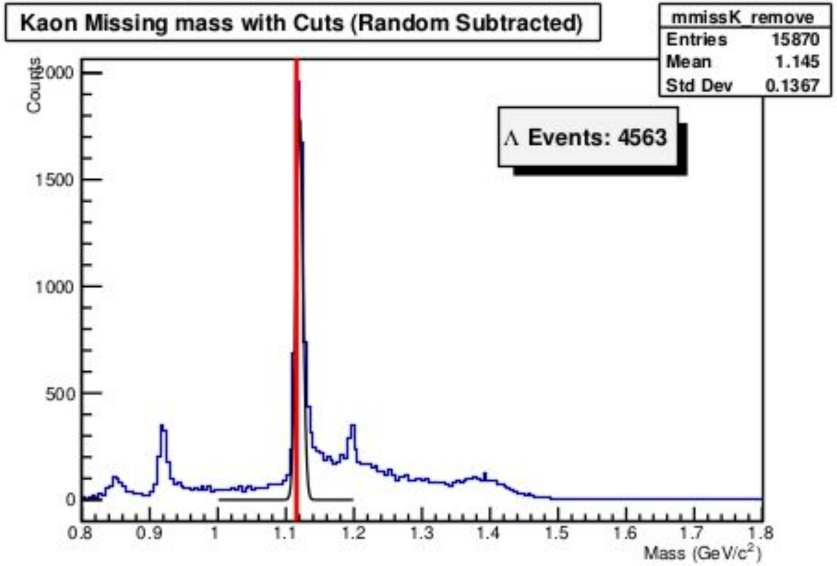

Comparison of high and low epsilon

- Q^2=4.4, W=2.74, x=0.40
- [10.6 Gev (high ε), 8.2 Gev (low ε)]
- Left (θ_{high}=15.81,θ_{low}=13.00)

10.6 GeV (high ε)

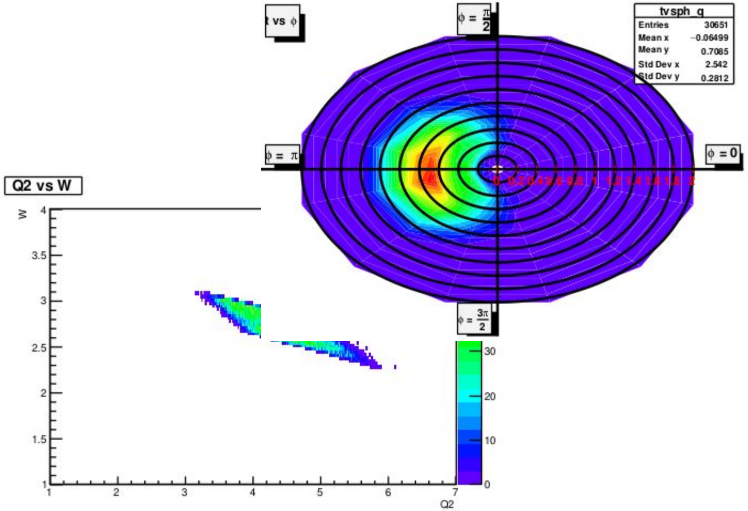

8.2 GeV (low ε)

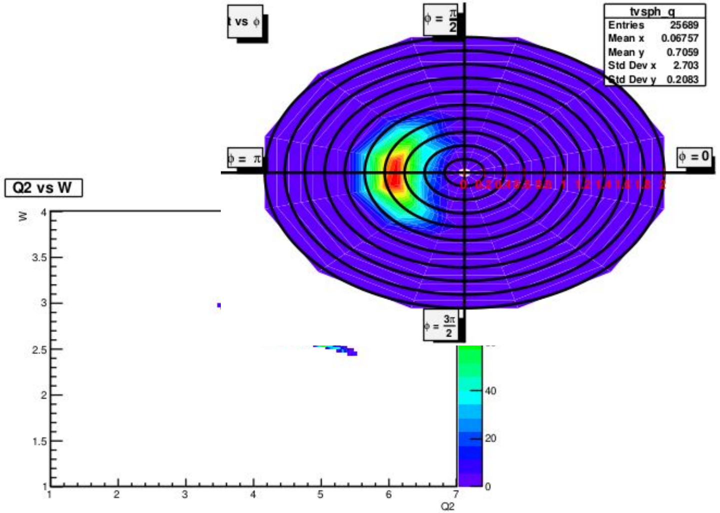

Comparison of high and low epsilon

- Q^2=4.4, W=2.74, x=0.40
- [10.6 Gev (high ε), 8.2 Gev (low ε)]
- Left (θ_{high}=15.81,θ_{low}=13.00)

10.6 GeV (high ε)

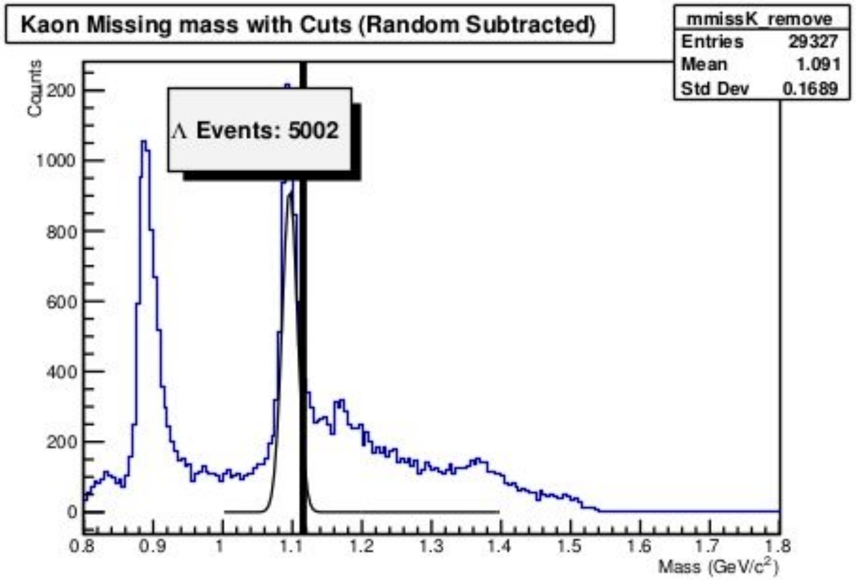

8.2 GeV (low ε)

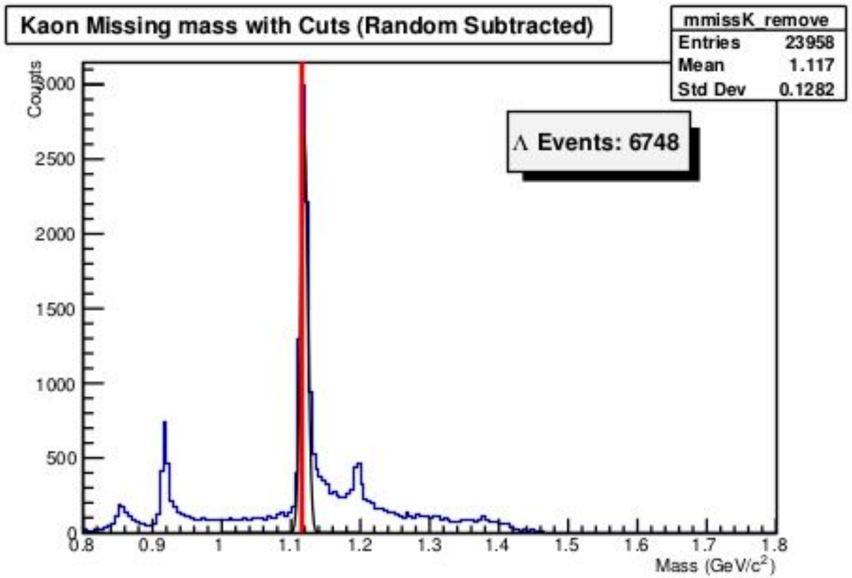

Comparison of high and low epsilon

- Q^2=4.4, W=2.74, x=0.40
- [10.6 Gev (high ε)]
- Right (θ_{high}=9.81)

10.6 GeV (high ε)

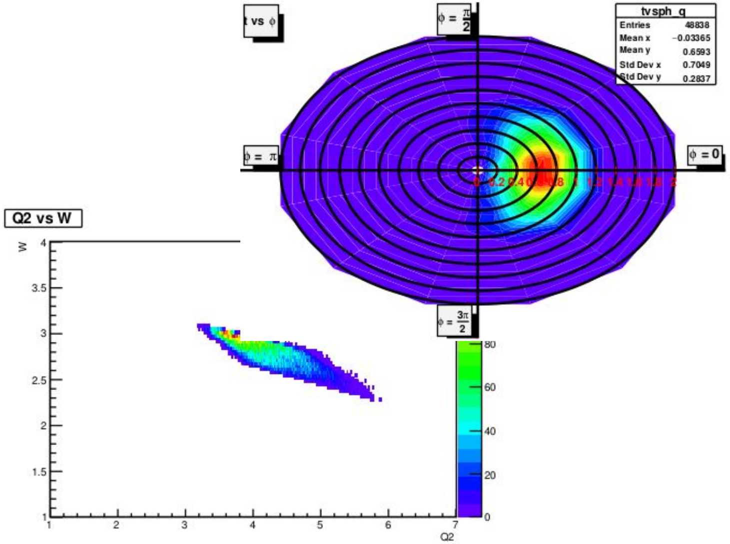

Comparison of high and low epsilon

- Q^2=4.4, W=2.74, x=0.40
- [10.6 Gev (high ε)]
- Right (θ_{high}=9.81)

10.6 GeV (high ε)

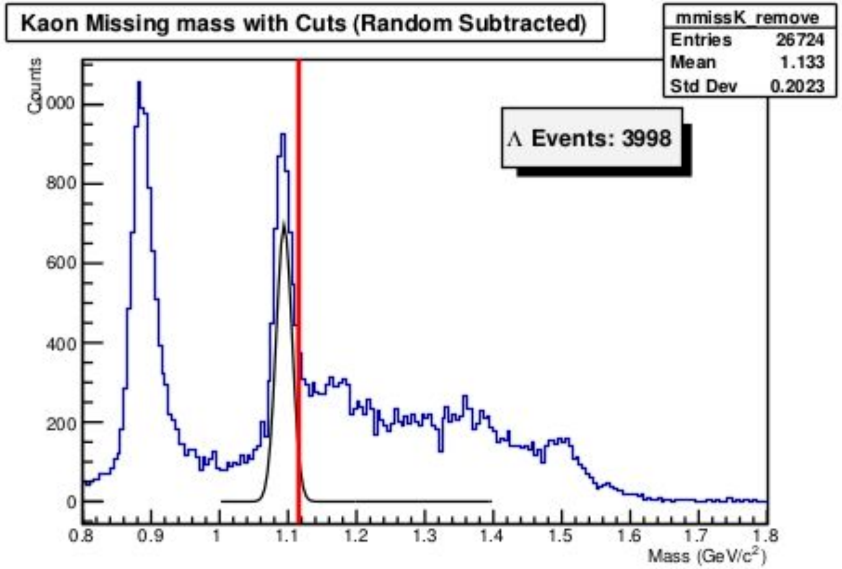

Comparison of high and low epsilon

- Q^2=3.0, W=3.14, x=0.25
- [10.6 Gev (high ε), 8.2 Gev (low ε)]
- Left (θ_{high}=12.42,θ_{low}=9.89)

10.6 GeV (high ε)

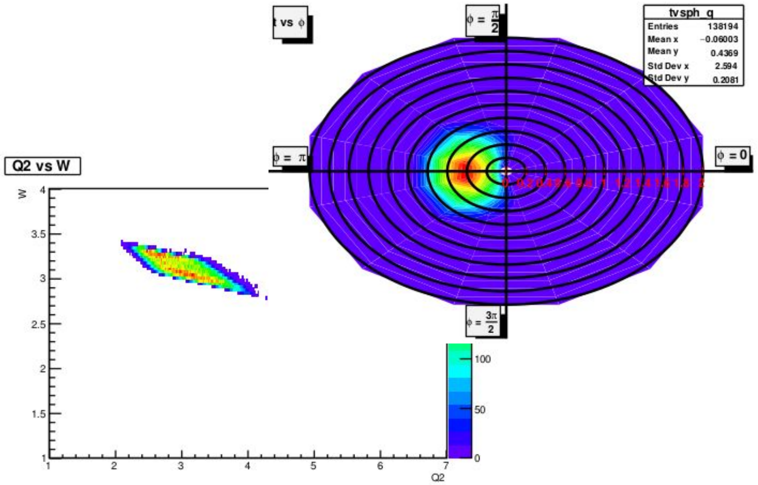

8.2 GeV (low ε)

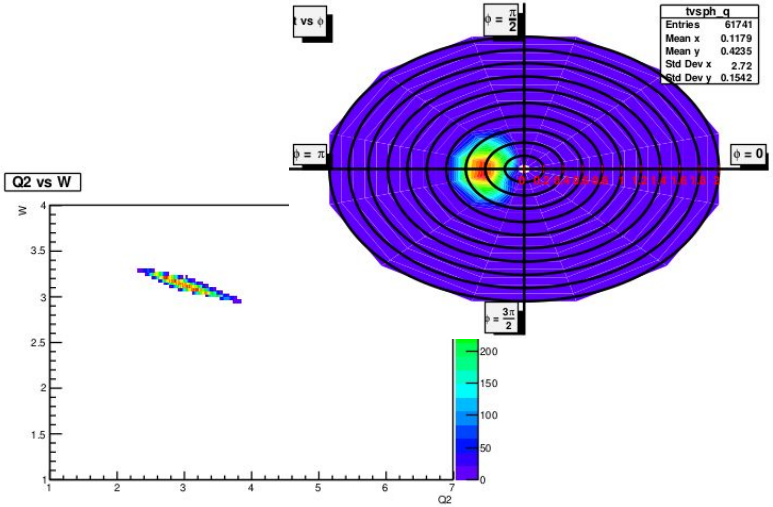

Comparison of high and low epsilon

- Q^2=3.0, W=3.14, x=0.25
- [10.6 Gev (high ε), 8.2 Gev (low ε)]
- Left (θ_{high}=12.42,θ_{low}=9.89)

10.6 GeV (high ε)

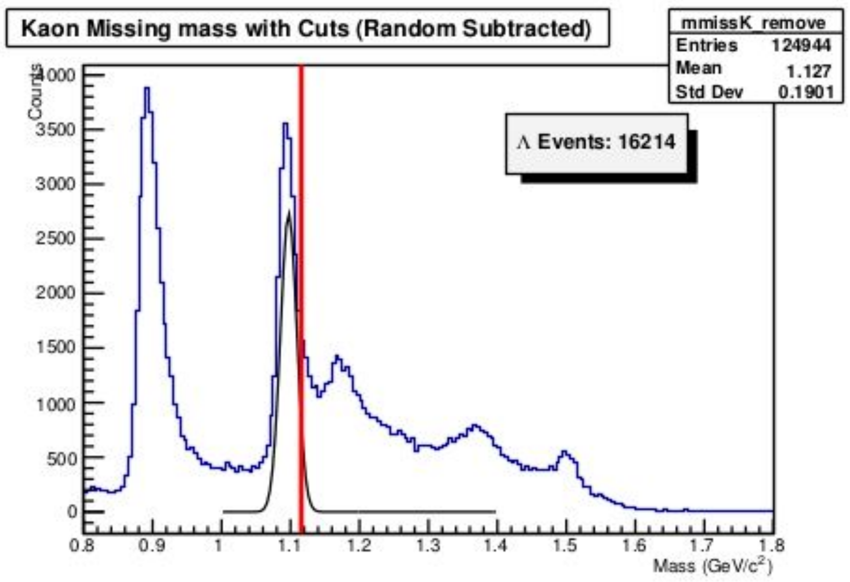

8.2 GeV (low ε)

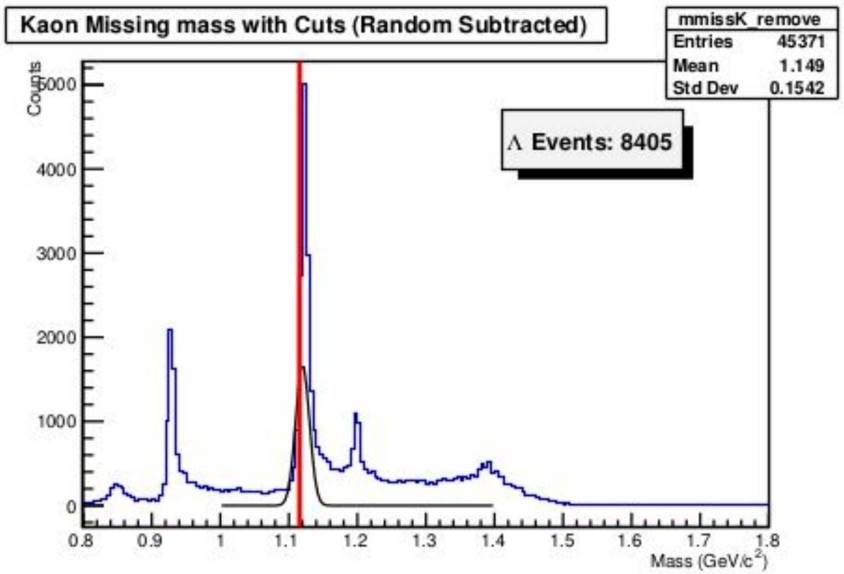

Comparison of high and low epsilon

- Q^2=5.5, W=3.02, x=0.40
- [10.6 Gev (high ε), 8.2 Gev (low ε)]
- Center (θ_{high}=9.56,θ_{low}=5.90)

10.6 GeV (high ε)

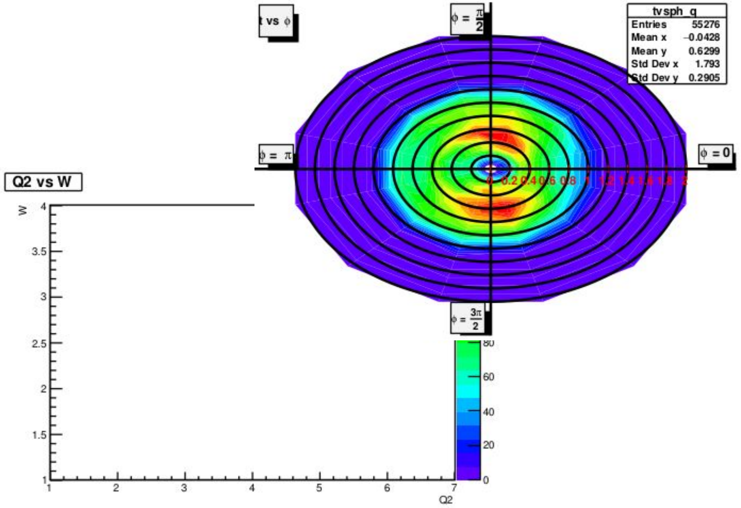

8.2 GeV (low ε)

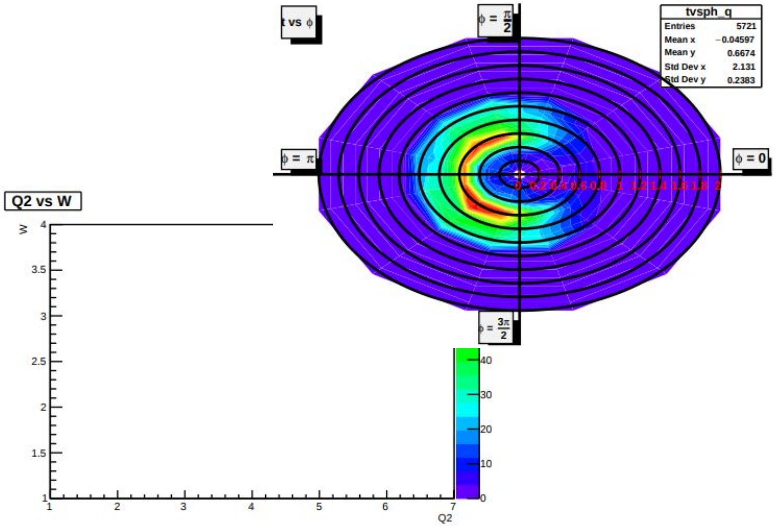

Comparison of high and low epsilon

- Q^2=5.5, W=3.02, x=0.40
- [10.6 Gev (high ε), 8.2 Gev (low ε)]
- Center (θ_{high}=9.56,θ_{low}=5.90)

10.6 GeV (high ε)

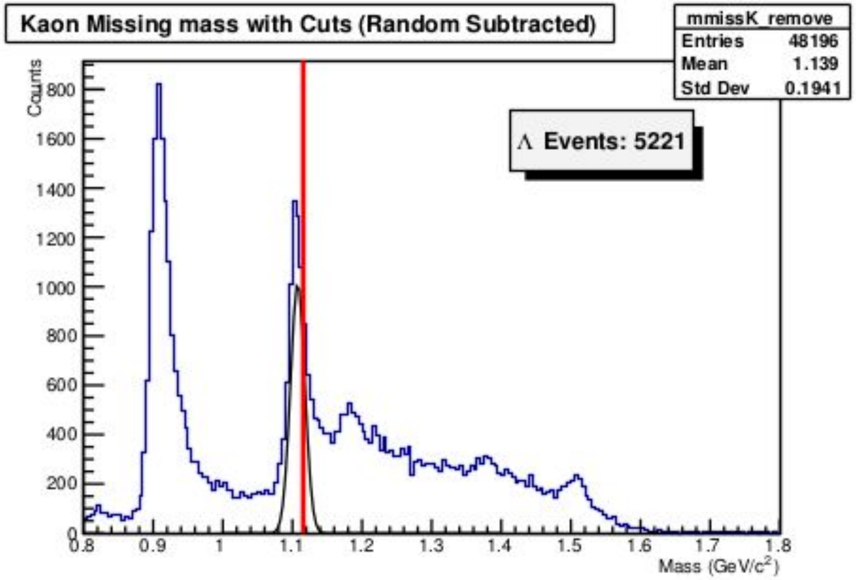

8.2 GeV (low ε)

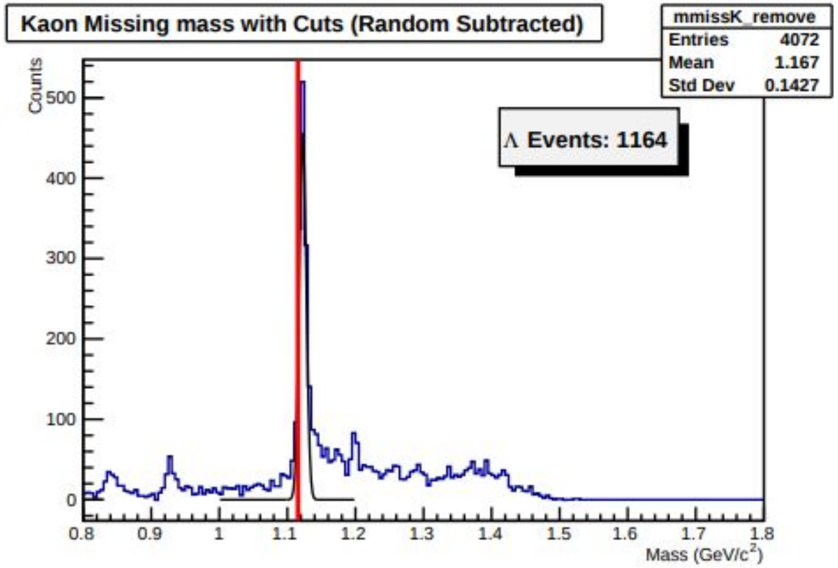

Comparison of high and low epsilon

- Q^2=5.5, W=3.02, x=0.40
- [10.6 Gev (high ε), 8.2 Gev (low ε)]
- Left (θ_{high}=12.56,θ_{low}=8.48)

10.6 GeV (high ε)

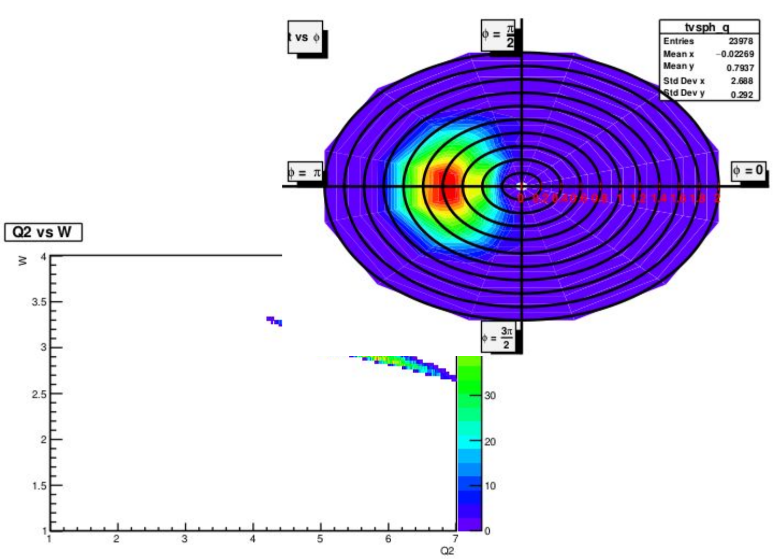

8.2 GeV (low ε)

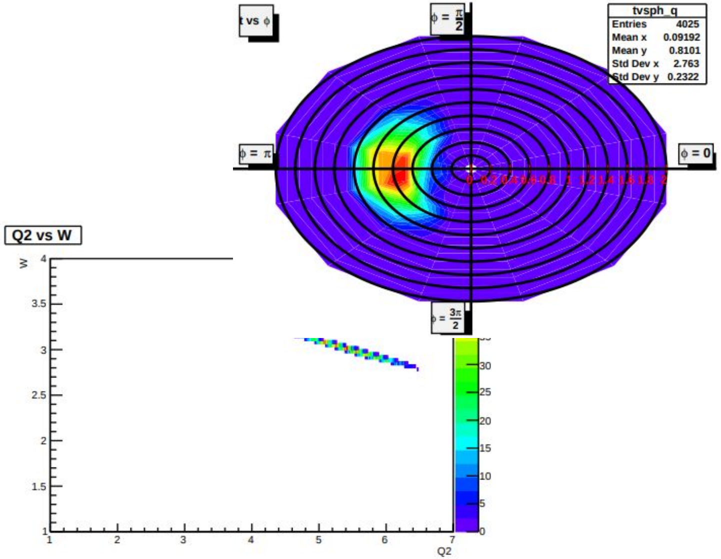

Comparison of high and low epsilon

- Q^2=5.5, W=3.02, x=0.40
- [10.6 Gev (high ε), 8.2 Gev (low ε)]
- Left (θ_{high}=12.56,θ_{low}=8.48)

10.6 GeV (high ε)

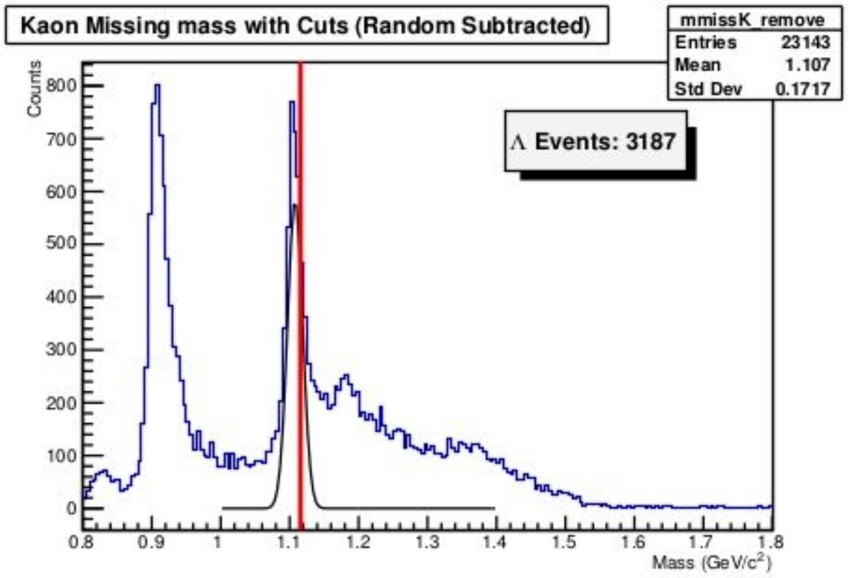

8.2 GeV (low ε)

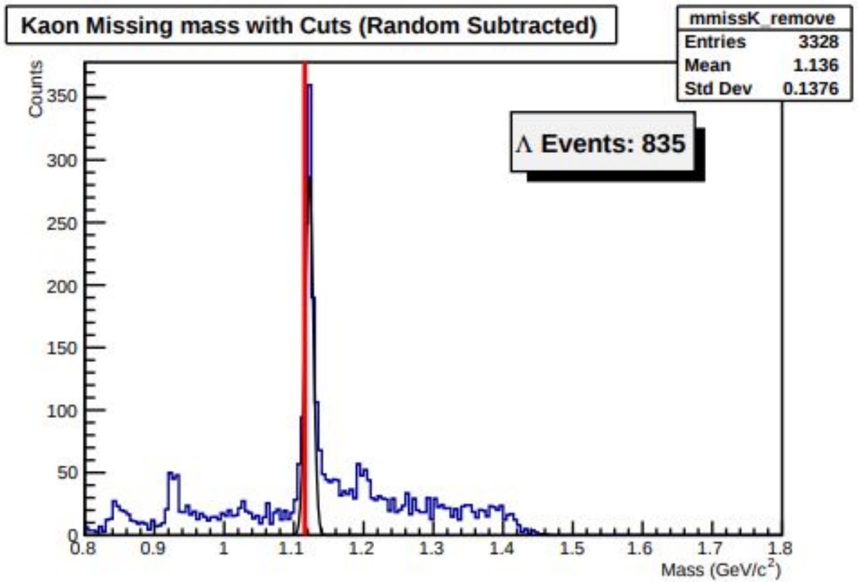

Comparison of high and low epsilon

- Q^2=5.5, W=3.02, x=0.40
- [10.6 Gev (high ε)]
- Right (θ_{high}=6.65)

10.6 GeV (high ε)

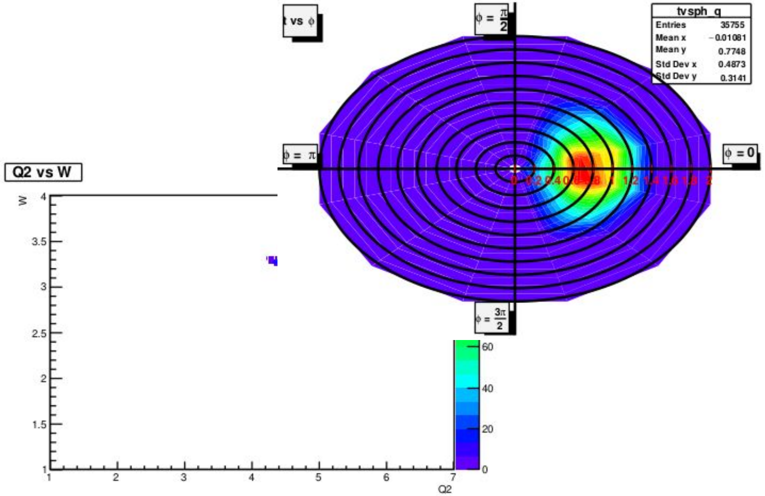

Comparison of high and low epsilon

- Q^2=5.5, W=3.02, x=0.40
- [10.6 Gev (high ε)]
- Right (θ_{high}=6.65)

10.6 GeV (high ε)

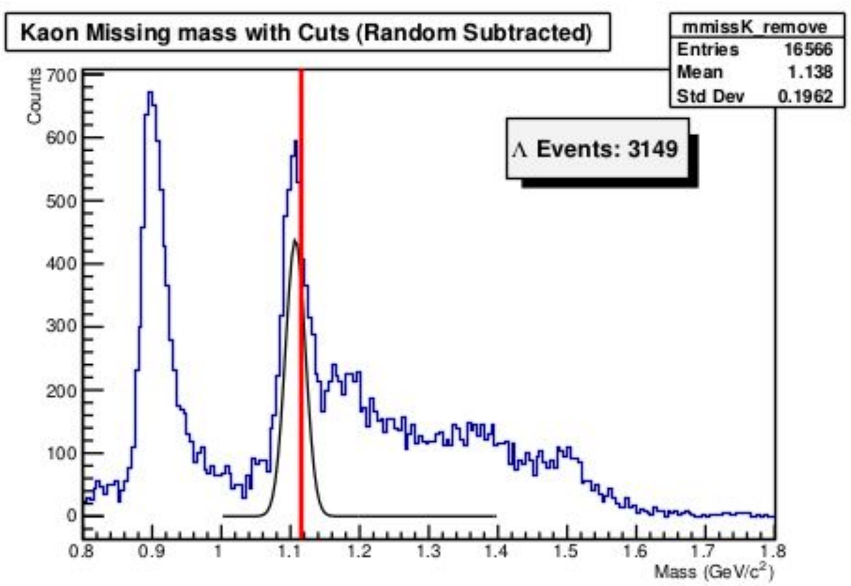

Comparison of high and low epsilon

- Q^2=0.5, W=2.40, x=0.09
- [4.9 Gev (high ε), 3.8 Gev (low ε)]
- Left (θ_{high}=11.86,θ_{low}=9.79)

4.9 GeV (high ε)

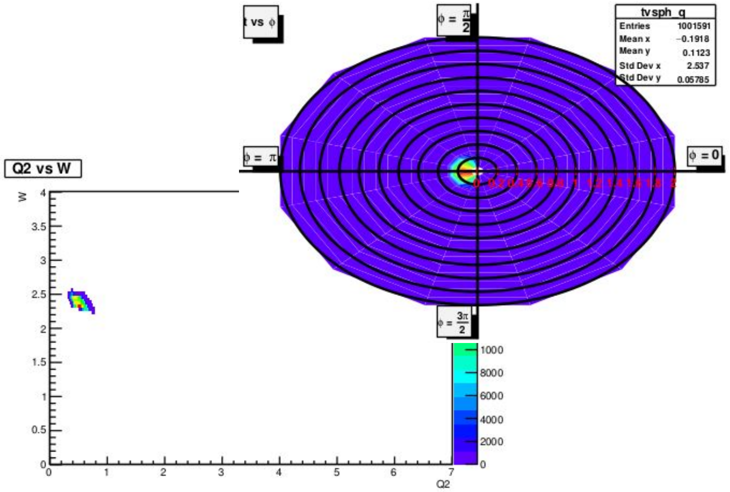

3.8 GeV (low ε)

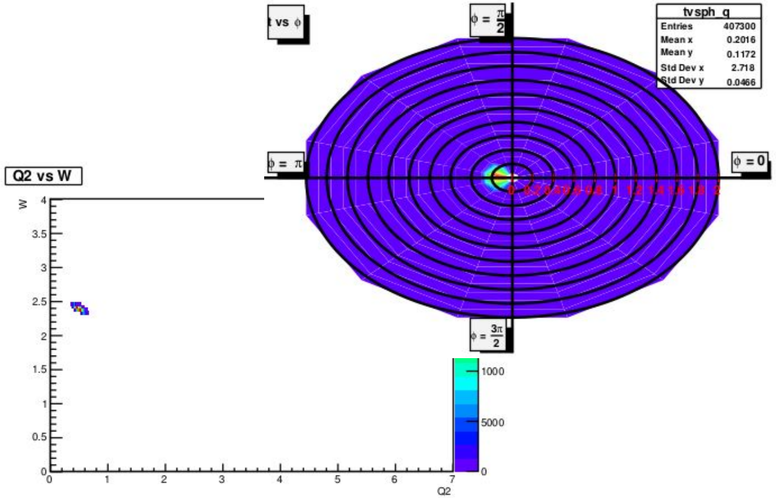

Comparison of high and low epsilon

- Q^2=0.5, W=2.40, x=0.09
- [4.9 Gev (high ε), 3.8 Gev (low ε)]
- Left (θ_{high}=11.86,θ_{low}=9.79)

4.9 GeV (high ε)

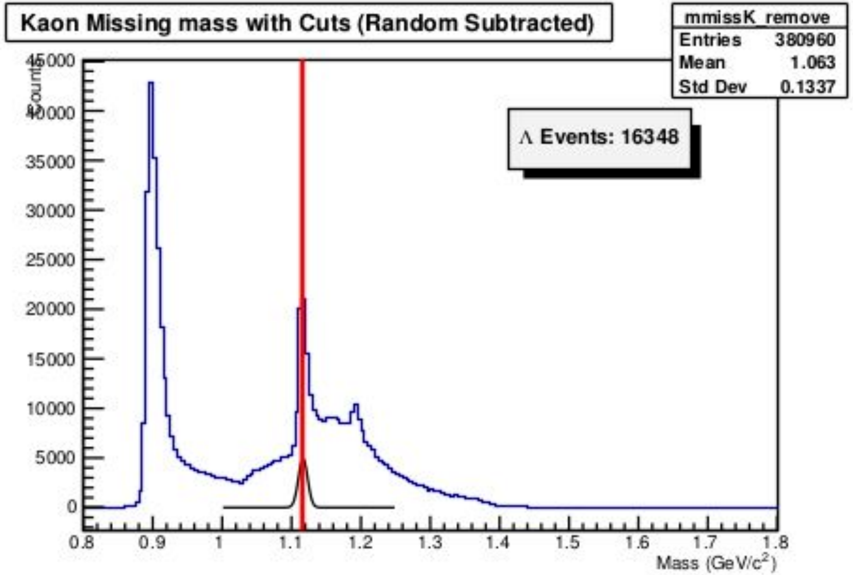

3.8 GeV (low ε)

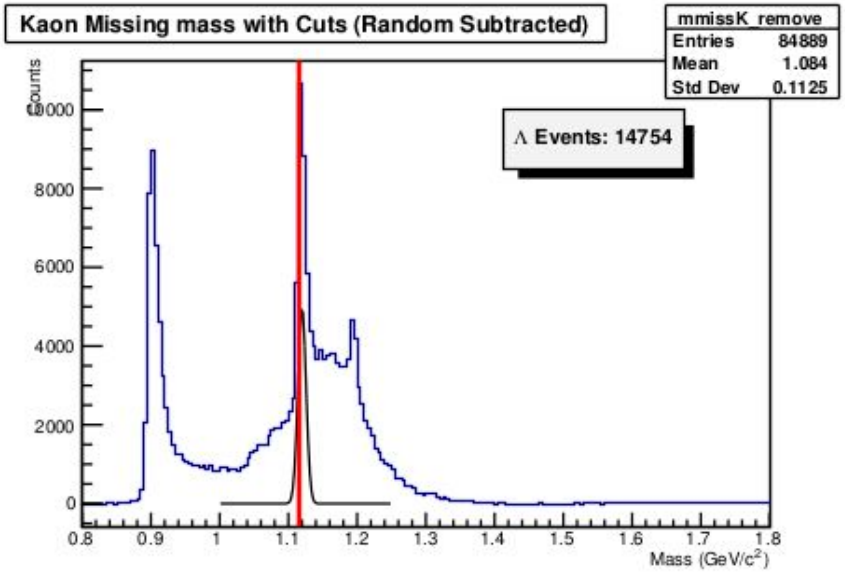

Comparison of high and low epsilon

- Q^2=0.5, W=2.40, x=0.09
- [4.9 Gev (high ε)]
- Right (θ_{high}=6.00)

4.9 GeV (high ε)

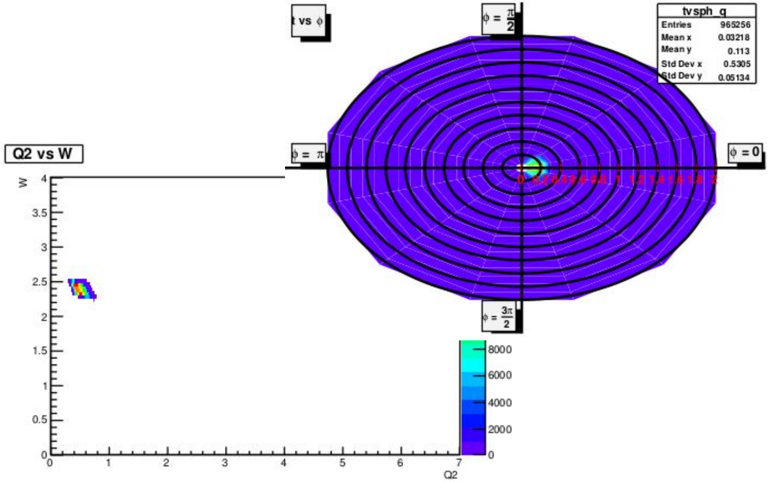

Comparison of high and low epsilon

- Q^2=0.5, W=2.40, x=0.09
- [4.9 Gev (high ε)]
- Right (θ_{high}=6.00)

4.9 GeV (high ε)